University of Maribor

UNIVERSITY OF THE WEST of SCOTLAND
UWS

10TH International Conference on Sustainable Energy and Environmental Protection:

Technical Developments in Vehicles

(June 27TH - 30TH, 2017, Bled, Slovenia)

(Conference Proceedings)

Editors:
Emeritus Prof. dr. Jurij Krope
Prof. dr. Abdul Ghani Olabi
Prof. dr. Darko Goričanec
Prof. dr. Stanislav Božičnik

University of Maribor Press


University of Maribor Press

10TH International Conference on Sustainable Energy and Environmental Protection

Technical Developments in Vehicles

(June 27TH – 30TH, 2017, Bled, Slovenia)

(Conference Proceedings)

Editors:
Emeritus Prof. dr. Jurij Krope
Prof. dr. Abdul Ghani Olabi
Prof. dr. Darko Goričanec
Prof. dr. Stanislav Božičnik

June 2017

Title: 10TH International Conference on Sustainable Energy and Environmental Protection (June 27TH – 30TH, 2017, Bled, Slovenia) (Conference Proceedings)

Subtitle: Technical Developments in Vehicles

Editors: Emeritus Prof. Jurij Krope, Ph.D. (University of Maribor, Slovenia),
Prof. Abdul Ghani Olabi, Ph.D. (University of the West of Scotland, UK),
Asso. Prof. Darko Goričanec, Ph.D. (University of Maribor, Slovenia),
Asso. Prof. Stanislav Božičnik (University of Maribor, Slovenia).

Review: Prof. Željko Knez, Ph.D. (University of Maribor, Slovenia),
Prof. Niko Samec, Ph.D. (University of Maribor, Slovenia).

Tehnical editors : Jan Perša (University of Maribor Press),
Armin Turanović (University of Maribor Press).

Design and layout: University of Maribor Press

Conference: 10TH International Conference on Sustainable Energy and Environmental Protection

First published in 2017 by
University of Maribor Press
Slomškov trg 15, 2000 Maribor, Slovenia
tel. +386 2 250 42 42, fax +386 2 252 32 45
http://press.um.si, zalozba@um.si

Co-published by
University of Maribor, Faculty of Chemistry and Chemical Engineering
Smetanova ulica 17,2000 Maribor, Slovenia
tel. +386 (0)2 22 94 400, faks + 386 (0)2 25 27 774
http://www.fkkt.um.si, fkkt@um.si

Published: 5. July 2017

CIP - Kataložni zapis o publikaciji
Univerzitetna knjižnica Maribor

629.33:001.892(082)(0.034.2)

INTERNATIONAL Conference on Sustainable Energy and Environmental Protection (10 ; 2017 ; Bled)
Technical developments in vehicles [Elektronski vir] : (Conference proceedings) / 10th International Conference on Sustainable Energy and Environmental Protection, (June 27th-30th, 2017, Bled, Slovenia) ; [organised by] University of Maribor [and] University of the West of Scotland ; editors Jurij Krope ... [et al.]. - El. zbornik. - Maribor : University of Maribor Press, 2017

Način dostopa (URL): http://press.um.si/index.php/ump/catalog/book/253

ISBN 978-961-286-062-2 (pdf)

doi: 10.18690/978-961-286-062-2
1. Gl. stv. nasl. 2. Krope, Jurij 3. Univerza (Maribor)
COBISS.SI-ID 92436225

ISBN 978-961-286-062-2

DOI: https://doi.org/10.18690/978-961-286-062-2

Price: Free copy

For publisher: Prof. Igor Tičar, Ph.D., rector (University of Maribor)

University of Maribor Press

Preface

The 10th International Conference on Sustainable Energy and environmental Protection – SEEP 2017 was organised on June 27th – 30th 2017 in Bled, Slovenia, by:

- Faculty of Chemistry and Chemical Engineering, University of Maribor, Slovenia,
- University of the West of Scotland, School of Engineering and

The aim of SEEP2017 is to bring together the researches within the field of sustainable energy and environmental protection from all over the world.

The contributed papers are grouped in 18 sessions in order to provide access to readers out of 300 contributions prepared by authors from 52 countries.

We thank the distinguished plenary and keynote speakers and chairs who have kindly consented to participate at this conference. We are also grateful to all the authors for their papers and to all committee members.

We believe that scientific results and professional debates shall not only be an incentive for development, but also for making new friendships and possible future scientific development projects.

General chair
Emeritus Prof. dr. Jurij Krope

10TH INTERNATIONAL CONFERENCE ON SUSTAINABLE ENERGY AND ENVIRONMENTAL PROTECTION (JUNE 27TH – 30TH, 2017, BLED, SLOVENIA), TECHNICAL DEVELOPMENTS IN VEHICLES
J. Krope, A.Ghani Olabi, D. Goričanec & S. Božičnik

Plenary Talk on
The Relation between Renewable Energy and Circular Economy

ABDUL GHANI OLABI - BIBLIOGRAPHY

Prof Olabi is director and founding member of the Institute of Engineering and Energy Technologies (www.uws.ac.uk\ieet) at the University of the West of Scotland. He received his M.Eng and Ph.D. from Dublin City University, since 1984 he worked at SSRC, HIAST, CNR, CRF, DCU and UWS. Prof Olabi has supervised postgraduate research students (10 M.Eng and 30PhD) to successful completion. Prof Olabi has edited 12 proceedings, and has published more than 135 papers in peer-reviewed international journals and about 135 papers in international conferences, in addition to 30 book chapters. In the last 12 months Prof Olabi has patented 2 innovative projects. Prof Olabi is the founder of the International Conference on Sustainable Energy and Environmental Protection SEEP, www.seepconference.co.uk

He is the Subject Editor of the Elsevier Energy Journal https://www.journals.elsevier.com/energy/editorial-board/abdul-ghani-olabi, also Subject editor of the Reference Module in Materials Science and Materials Engineering http://scitechconnect.elsevier.com/reference-module-material-science/ and board member of a few other journals. Prof Olabi has coordinated different National, EU and International Projects. He has produced different reports to the Irish Gov. regarding: Hydrogen and Fuel Cells and Solar Energy.

CORRESPONDENCE ADDRESS: Abdul Ghani Olabi, Ph.D., Professor, University of the West of Scotland, School of Engineering and Computing, D163a, McLachlan Building, Paisley, United Kingdom, e-mail: Abdul.Olabi@uws.ac.uk.

https://doi.org/10.18690/978-961-286-062-2 ISBN 978-961-286-062-2

Available at: http://press.um.si.

10TH INTERNATIONAL CONFERENCE ON SUSTAINABLE ENERGY AND ENVIRONMENTAL PROTECTION (JUNE 27TH – 30TH, 2017, BLED, SLOVENIA), TECHNICAL DEVELOPMENTS IN VEHICLES
J. Krope, A.Ghani Olabi, D. Goričanec & S. Božičnik

University of Maribor Press

Plenary Talk on Energy Footprints Reduction and Virtual Footprints Interactions

JIŘÍ JAROMÍR KLEMEŠ & PETAR SABEV VARBANOV

Increasing efforts and resources have been devoted to research during environmental studies, including the assessment of various harmful impacts from industrial, civic, business, transportation and other economy activities. Environmental impacts are usually quantified through Life Cycle Assessment (LCA). In recent years, footprints have emerged as efficient and useful indicators to use within LCA. The footprint assessment techniques has provided a set of tools enabling the evaluation of Greenhouse Gas (GHG) – including CO_2, emissions and the corresponding effective flows on the world scale. From all such indicators, the energy footprint represents the area of forest that would be required to absorb the GHG emissions resulting from the energy consumption required for a certain activity, excluding the proportion absorbed by the oceans, and the area occupied by hydroelectric dams and reservoirs for hydropower.

An overview of the virtual GHG flow trends in the international trade, associating the GHG and water footprints with the consumption of goods and services is performed. Several important indications have been obtained: (a) There are significant GHG gaps between producer's and consumer's emissions – US and EU have high absolute net imports GHG budget. (b) China is an exporting country and increasingly carries a load of GHG emission and virtual water export associated with consumption in the relevant importing countries. (c) International trade can reduce global environmental pressure by redirecting import to products produced with lower intensity of GHG emissions and lower water footprints, or producing them domestically.

To develop self-sufficient regions based on more efficient processes by combining neighbouring countries can be a promising development. A future direction should be focused on two main areas: (1) To provide the self-sufficient regions based on more efficient processes by combining production of surrounding countries. (2) To develop the shared mechanism and market share of virtual carbon between trading partners regionally and internationally.

CORRESPONDENCE ADDRESS: Jiří Jaromír Klemeš, DSc, Professor, Brno University of Technology - VUT Brno, Faculty of Mechanical Engineering, NETME Centre, Sustainable Process Integration Laboratory – SPIL, Technická 2896/2, 616 69 Brno, Czech Republic, e-mail: klemes@fme.vutbr.cz. Petar Sabev Varbanov, Ph.D., Associate Professor, Brno University of Technology - VUT Brno, Faculty of Mechanical Engineering, NETME Centre, Sustainable Process Integration Laboratory – SPIL, Technická 2896/2, 616 69 Brno, Czech Republic, e-mail: varbanov@fme.vutbr.cz.

https://doi.org/10.18690/978-961-286-062-2 ISBN 978-961-286-062-2

Available at: http://press.um.si.

University of Maribor Press

JIŘÍ JAROMÍR KLEMEŠ - BIBLIOGRAPHY

Head of "Sustainable Process Integration Laboratory – SPIL", NETME Centre, Faculty of Mechanical Engineering, Brno University of Technology - VUT Brno, Czech Republic and Emeritus Professor at "Centre for Process Systems Engineering and Sustainability", Pázmány Péter Catholic University, Budapest, Hungary.

Previously the Project Director, Senior Project Officer and Hon Reader at Department of Process Integration at UMIST, The University of Manchester and University of Edinburgh, UK. Founder and a long term Head of the Centre for Process Integration and Intensification – CPI2, University of Pannonia, Veszprém, Hungary. Awarded by the EC with Marie Curies Chair of Excellence (EXC). Track record of managing and coordinating 91 major EC, NATO and UK Know-How projects. Research funding attracted over 21 M€.

Co-Editor-in-Chief of Journal of Cleaner Production (IF=4.959). The founder and President for 20 y of PRES (Process Integration for Energy Saving and Pollution Reduction) conferences. Chairperson of CAPE Working Party of EFCE, a member of WP on Process Intensification and of the EFCE Sustainability platform.

He authored nearly 400 papers, h-index 40. A number of books published by McGraw-Hill; Woodhead; Elsevier; Ashgate Publishing Cambridge; Springer; WILEY-VCH; Taylor & Francis).

Several times Distinguished Visiting Professor for Universiti Teknologi Malaysia, Xi'an Jiaotong University; South China University of Technology, Guangzhou; Tianjin University in China; University of Maribor, Slovenia; University Technology Petronas, Malaysia; Brno University of Technology and the Russian Mendeleev University of Chemical Technology, Moscow. Doctor Honoris Causa of Kharkiv National University "Kharkiv Polytechnic Institute" in Ukraine, the University of Maribor in Slovenia, University POLITEHNICA Bucharest, Romania. "Honorary Doctor of Engineering Universiti Teknologi Malaysia", "Honorary Membership of Czech Society of Chemical Engineering", "European Federation of Chemical Engineering (EFCE) Life-Time Achievements Award" and "Pro Universitaire Pannonica" Gold Medal.

CORRESPONDENCE ADDRESS: Jiří Jaromír Klemeš, DSc, Professor, Brno University of Technology - VUT Brno, Faculty of Mechanical Engineering, NETME Centre, Sustainable Process Integration Laboratory – SPIL, Technická 2896/2, 616 69 Brno, Czech Republic, e-mail: klemes@fme.vutbr.cz.

https://doi.org/10.18690/978-961-286-062-2 ISBN 978-961-286-062-2

Available at: http://press.um.si.

10TH INTERNATIONAL CONFERENCE ON SUSTAINABLE ENERGY AND ENVIRONMENTAL PROTECTION (JUNE 27TH – 30TH, 2017, BLED, SLOVENIA), TECHNICAL DEVELOPMENTS IN VEHICLES
J. Krope, A.Ghani Olabi, D. Goričanec & S. Božičnik

University of Maribor Press

Plenary Talk on Renewable energy sources for environmental protection

HAKAN SERHAD SOYHAN

Development in energy sector, technological advancements, production and consumption amounts in the countries and environmental awareness give shape to industry of energy. When the dependency is taken into account in terms of natural resources and energy, there are many risks for countries having no fossil energy sources. Renewable and clean sources of energy and optimal use of these resources minimize environmental impacts, produce minimum secondary wastes and are sustainable based on current and future economic and social societal needs. Sun is one of the main energy sources in recent years. Light and heat of sun are used in many ways to renewable energy. Other commonly used are biomass and wind energy. To be able to use these sources efficiently national energy and natural resources policies should be evaluated together with the global developments and they should be compatible with technological improvements. Strategic plans with regard to energy are needed more intensively and they must be in the qualification of a road map, taking into account the developments related to natural resources and energy, its specific needs and defining the sources owned by countries. In this presentation, the role of supply security was evaluated in term of energy policies. In this talk, new technologies in renewable energy production will be shown and the importance of supply security in strategic energy plan will be explained.

CORRESPONDENCE ADDRESS: Hakan Serhad Soyhan, Ph.D., Professor, Sakarya University, Engineering Faculty, Esentepe Campus, M7 Building, 54187 - Esentepe /Sakarya, Turkey, e-mail: hsoyhan@sakarya.edu.tr.

https://doi.org/10.18690/978-961-286-062-2 ISBN 978-961-286-062-2

Available at: http://press.um.si.

University of Maribor Press

HAKAN SERHAD SOYHAN - BIBLIOGRAPHY

Professor at Sakarya University, Engineering Faculty. 50 % fot teaching and the rest for reasearch activities.

Teaching, courses taught:

Graduate courses:

- Combustion technology;
- Modelling techniques;

Undergraduate courses:

- Combustion techniques;
- Internal combustion engines;
- Fire safety.

Tehnical skills and competences professional societies:

- 25 jurnal papers in SCI Index. 23 conference papers;
- Editor at FCE journal. Co-editor at J of Sakarya University;
- Head of Local Energy Research Society (YETA);
- Member od American Society of Mechanical engineers (ASME);
- Member of Turkish Society of Mechanical Engineers (TSME).

CORRESPONDENCE ADDRESS: Hakan Serhad Soyhan, Ph.D., Professor, Sakarya University, Engineering Faculty, Esentepe Campus, M7 Building, 54187 - Esentepe /Sakarya, Turkey, e-mail: hsoyhan@sakarya.edu.tr.

https://doi.org/10.18690/978-961-286-062-2 ISBN 978-961-286-062-2

Available at: http://press.um.si.

University of Maribor Press

Table of Contents

CONFERENCE PROCEEDINGS

10TH INTERNATIONAL CONFERENCE ON SUSTAINABLE ENERGY AND ENVIRONMENTAL PROTECTION (JUNE 27TH – 30TH, 2017, BLED, SLOVENIA), TECHNICAL DEVELOPMENTS IN VEHICLES
J. Krope, A.Ghani Olabi, D. Goričanec & S. Božičnik

Robust Neuro-Fuzzy Sliding Mode Speed Control for an Electric Drive System

IBRAHIM FAROUK BOUGUENNA, AHMED AZAIZ, AHMED TAHOUR & AHMED LARBAOUI

Abstract This work present a Robust Neuro-fuzzy-sliding mode speed control (NFSMC) to ensure the traction of an electric vehicle; at the first we applied the sliding mode control (SMC) on the three surfaces speed, direct current and quadrature current on the permanent magnet synchronous motor PMSM by taking into account the dynamics of the vehicle; And afterwards we applied the Neuro-fuzzy-sliding mode on the speed surface ; Simulation under Matlab/Simulink has been carried out to evaluate the efficiency and robustness of the proposed control on a system drive. It should be noted that the reference speed is the European urban driving schedule ECE-15 cycle.

Keywords: • Electric vehicle • Sliding mode control • Neuro-Fuzzy • PMSM • Dynamics •

CORRESPONDENCE ADDRESS: Ibrahim Farouk Bouguenna, PhD student, University of Sidi Bel abbes, Faculty of electrical Engineering ,22000 Sidi Bel Abbes, Algeria, e-mail:faroukspvusto@yahoo.fr. Ahmed Azaiz, Ph.D., Full Professor, University of Sidi Bel abbes, Faculty of electrical Engineering ,22000 Sidi Bel Abbes, Algeria, e-mail: ahazaiz2011@yahoo.fr. Ahmed Tahour, Ph.D., Full Professor, University of Sidi Bel abbes, Faculty of electrical Engineering ,22000 Sidi Bel Abbes, Algeria, e-mail: tahourahmed@yahoo.fr. Ahmed Larbaoui, PhD Student, University of Sidi Bel abbes, Faculty of electrical Engineering ,22000 Sidi Bel Abbes, Algeria, e-mail: s.godounov@gmail.com.

https://doi.org/10.18690/978-961-286-062-2.1 ISBN 978-961-286-062-2

Available at: http://press.um.si.

1 Introduction

Due to the increasing requirements with regard to introducing environmental-friendly vehicles and electrification of vehicle systems, much research on electric vehicles has been carried out [1]. In particular control system as electric vehicle's brain which is a very important part of the whole system and, to a great extent, determines the entire vehicle performance, as it is the key to improve motor efficiency. in this context a Permanent magnet synchronous motor has been adopted as the electric vehicle (EV) propulsion.

The FIS forms are a useful computing framework based on the concepts of fuzzy set theory, fuzzy if–then rules and fuzzy reasoning. The ANFIS [2, 3] is a FIS implemented in the framework of an adaptive fuzzy neural network. It combines the explicit knowledge representation of a FIS with the learning power of ANNs. Usually, the transformation of human knowledge into a fuzzy system (in the form of rules and membership functions) does not give the target response accurately. So, the parameters of the FIS should be determined optimally [4].

The reminder of this paper is organized as follows: section 2 reviews the principle components of the traction system and their model equations. Section 3 shows the development of sliding mode controllers for electric vehicle motorization. Section 4 shows the proposed Neuro-fuzzy-sliding mode control law model to remedy the chattering phenomena. Section 5 a simulation results verify the validity of the proposed method of control. Finally the conclusion is drawn in section 6 .

2 Electric vehicle traction system modeling

This part is devoted to the dynamics of the electric vehicle and the different components on board the vehicle and their equations models.

2.1 Vehicle Dynamics

The elementary equation describing the longitudinal dynamics of a vehicle in the road is in the following form:

$$m_v \frac{d}{dt} v(t) = F_t(t) - (F_{ad}(t) + F_{rr}(t) + F_g(t)) \quad (1)$$

Consider a vehicle of mass, m_v proceeding at a velocity v, up a slope of angle α, coefficient of rolling resistance C_{rr} , density of the air ρ, frontal surface of the vehicle A_f, coefficient of penetration into the air C_d .

The force propelling the vehicle forward F_t, the tractive effort, has to accomplish the following [5-7]:

- overbear the rolling resistance:

$$F_{rr} = C_{rr}.m_v.g.\cos(\alpha) \tag{2}$$

- overbear the aerodynamic drag:

$$F_{ad} = \frac{1}{2}.\rho.A_f.C_d.(v - v_0)^2 \tag{3}$$

- provide the force needed to overcome the component of the vehicle's weight acting down the slope:

$$F_g = \pm m_v.g.\sin(\alpha) \tag{4}$$

- accelerate the vehicle, if the velocity is not constant:

$$F_{acc} = m_v.\frac{d}{dt}.v(t) \tag{5}$$

2.2 Mathematical model of the PMSM

In this work we use a three phase induction motor type PMSM In the stationary (d − q) reference frame, the mathematics mode of permanent-magnet synchronous motor is shown as below [8]-[9]:

$$\begin{cases} i_d^{\bullet} = -\dfrac{R_s}{L_d} i_d + \dfrac{L_q}{L_d} p\omega_r i_q + \dfrac{1}{L_d} u_d \\ i_q^{\bullet} = -\dfrac{R_s}{L_q} i_q - \dfrac{L_d}{L_q} p\omega_r i_d - \dfrac{p\psi_f}{L_q} \omega_r + \dfrac{1}{L_q} u_q \\ \omega_r^{\bullet} = \dfrac{p(L_d - L_q) i_d + p\psi_f}{J} i_q - \dfrac{1}{J} C_r - \dfrac{f}{J} \omega_r \end{cases} \tag{6}$$

With R_s :Stator resistance, L_d , L_q d and q axis stator inductances ψ_f :Permanent-magnet flux linkage, i_d , i_q : Stator currents, u_q : Stator voltages, ω_r : Speed mechanic, j : Moment of inertia, f : Coefficient of viscous friction, p : Number of pole pairs, C_r : Load torque.

3 Sliding mode control design for PMSM

Sliding modes is phenomenon may appear in a dynamic system governed by ordinary differential equations with discontinuous right-hand sides. It may happen that the control as a function of the system state switches at high frequency, this motion is called sliding mode.

SMC has its own disadvantage, i.e., chattering phenomenon, which originated from the interaction between parasitic dynamics and high frequency switching control. In order to avoid the phenomenon, several control methods were proposed in the literature [10] [11].

3.1 Three surface control strategy

We take the general equation Proposed by J.J.Slotine to determine the sliding surface :

$$s(x,t)=\left(\frac{\partial}{\partial t}+\lambda\right)^{(n-1)}.e \tag{7}$$

s : the sliding surface
e : Error of the quantity to be controlled,
λ : Vector of slopes of the s ,
$_n$: Relative degree, equal to the number of times it derives the output for the command to appear.

Figure 1 shows scheme of the sliding mode control of the electric traction system using the principle of the cascade control method, the structure comprises a speed control loop which generates the current reference i_{qref} which imposes the control v_{qref} , the control v_{dref} is imposed by the current regulation i_{dref} .

3.1.1 Direct axis control design

The resulting error will be corrected by a regulator operating in the sliding mode and the surface of this control is given by:

$$s_1 = i_{dref} - i_d \tag{8}$$

Considering the expression of the current i_d deducted in the equation system Eq. (6), the derivative of the surface becomes:

$$s_1^{\bullet} = i_{dref}^{\bullet} + \frac{R_s}{L_d} i_d - \frac{L_q}{L_d} p\omega_r i_q - \frac{1}{L_d} u_d \tag{9}$$

During the sliding mode we have $s^{\bullet}(i_d) = 0, U_{qN} = 0$

$$U_{deq} = (i_{dref}^{\bullet} + \frac{R_s}{L_d} i_d - \frac{L_q}{L_d} p\omega_r i_q) L_d \tag{10}$$

$$U_{dN} = K_d sign(s(i_d)) \tag{11}$$

Where : k_d is positive gain for the direct current regulator.

3.1.2 Quadrature axis control design

The surface of this control is given by the following equation:

$$s_2 = i_{qref} - i_q \tag{12}$$

The derivative of the surface becomes:

$$s_2^{\bullet} = i_{qref}^{\bullet} - (-\frac{R_s}{L_q} i_q - \frac{L_d}{L_q} p\omega_r i_d - \frac{p\psi_f}{L_q} \omega_r + \frac{1}{L_q} u_q) \tag{13}$$

During the sliding mode we have $s^{\bullet}(i_q) = 0, s(i_q) = 0, U_{qN} = 0$

$$U_{qeq} = (i^{\bullet}_{qref} + \frac{R_s}{L_q} i_q + \frac{L_d}{L_q} p\omega_r i_d + \frac{p\psi_f}{L_q} \omega_r) L_q \tag{14}$$

$$U_{qN} = K_q sign(s(i_q)) \tag{15}$$

Where : k_q is positive gain for the quadrature current regulator.

3.1.3 Speed controller

$$s = \omega_{rref} - \omega_r \tag{16}$$

By replacing Eq. (c) in Eq. (20), we obtain:

$$s^{\bullet} = \omega^{\bullet}_{rref} - \frac{p(L_d - L_q) i_d + p\psi_f}{J} i_q + \frac{1}{J} C_r + \frac{f}{J} \omega_r \tag{17}$$

During the sliding mode we have $s^{\bullet}(\omega_r) = 0, s(\omega_r) = 0, i_{qN} = 0$

$$i_{qeq} = \frac{\omega^{\bullet}_{rref} + \frac{f}{J}\omega_r + \frac{1}{J} C_r}{\frac{p(L_d - L_q)}{J} i_d + p\frac{\psi_f}{J}} \tag{18}$$

$$i_{qN} = K_{\omega_r} sign(s(\omega_r)) \tag{19}$$

with : K_{ω_r} is positive gain for the speed controller.

4 Adaptative neuro-fuzzy mode speed controller

The disadvantage of sliding mode controllers is that the discontinuous control signal produces chattering dynamics, for this reason the combination of neural network with the fuzzy logic control (FLC) aims to improve the robustness and the performance of the controlled nonlinear systems. The proposed Neuro-fuzzy-sliding mode control (NFSMC) scheme for electric vehicle (EV) speed control is shown in Figure 2. The Neuro-fuzzy logic controller replace the speed surface sliding mode.

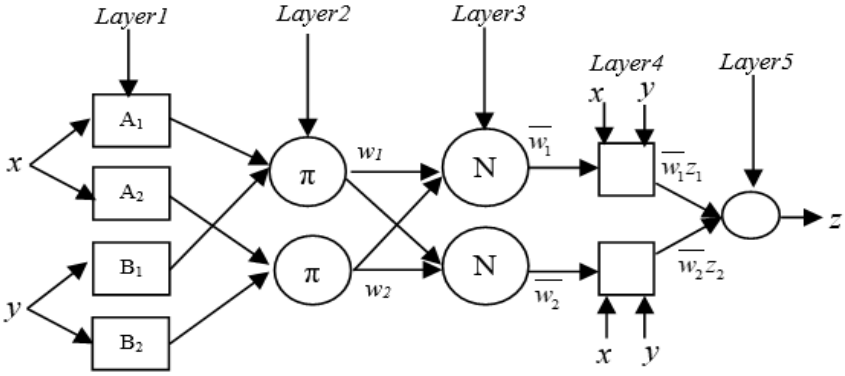

Figure 2. Block diagram of proposed Adaptative Neuro-fuzzy sliding mode control speed

A typical architecture of an ANFIS is shown in Figure 3, in which a circle indicates a fixed node, whereas a square indicates an adaptive node. For simplicity, we consider two inputs x, y and one output z. Among many FIS models, the Sugeno fuzzy model is the most widely applied one for its high interpretability and computational efficiency, and built-in optimal and adaptive techniques [2].

Figure 3. Architecture of ANFIS

The ANFIS controller generates change in the reference current (i_{qref}), based on speed error (e) defined as [4]:

$$e = \omega_{rref} - \omega_r \tag{20}$$

Where ω_{rref} and ω_r are the reference and the actual speeds, respectively.

In this study first order Sugeno type fuzzy inference was used for ANFIS and the typical fuzzy rule is:
if e is A_i and de is B_i then $z=f(e)$

Where A and B are fuzzy sets in the antecedent and $z=f(e)$ is a crisp function in the consequent.

The significances of ANFIS structure are:

Layer 1: Each adaptive node in this layer generates the membership grades for the input vectors A_i, i=1,…,3. In this paper, the node function is a triangular membership function:

$$O_i^1 = \mu_{Ai}(e) = \begin{cases} 0 & e \le a_i \\ \dfrac{e-a_i}{b_i-a_i} & a_i \le e \le b_i \\ \dfrac{c-e}{c-b_i} & b_i \le e \le c_i \\ 0 & c_i \le e \end{cases} \tag{21}$$

Layer 2: The total number of rule is 9 in this layer. Each node output represents the activation level of a rule:

$$O_i^1 = w_i = \min((\mu_{Ai}(e)) \quad i = 1....3 \tag{22}$$

*layer 3:*Fixed node i in this layer calculate the ratio of the i-th rule's activation level to the total of all activation level:

$$O_i^3 = \overline{w_i} = \frac{w}{\sum_{j=1}^{n} w_j} \tag{23}$$

Layer 4: Adaptive node i in this layer calculate the contribution of i-th rule towards the overall output, with the following node function:

$$O_i^4 = \overline{w_i} z_i = \overline{w_i}(p_i e + r_i) \tag{24}$$

Layer 5: The single fixed node in this layer computes the overall output as the summation of contribution from each rule:

$$O_i^5 = \sum_{i=1}^{2} \overline{w}_i z_i = \frac{w_1 z_1 + w_2 z_2}{w_1 + w_2} \tag{25}$$

The parameters to be trained are, a_i, b_i, and c_i of the premise parameters and p_i and r_i of the consequent parameters. Training algorithm requires a training set defined between inputs and output [4][12].

5 Simulation results

In order to control the vehicle traction system behavior, simulations were carried out. They show the vehicle speed control using sliding mode controllers (SMC) and Neuro-fuzzy sliding mode controllers (NFMSC).

It should be noted that the simulation run under European urban driving cycle ECE-15, during this cycle three trapezoids speed (9 km/h, 19 km/h, 30 km/h) shall be requested by the driver. In addition we applied a slope of 10% between 16s and 23s. The purpose of this simulation mode is to test our control technique through a real driving cycle.

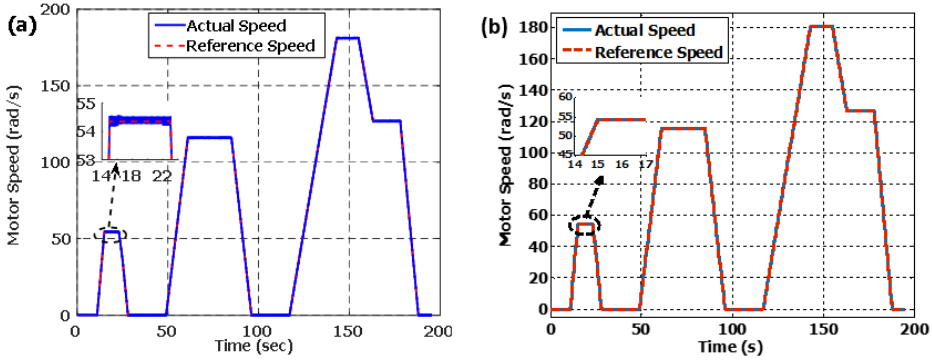

Figure 4. Motor Speed (SMC & NFSMC)

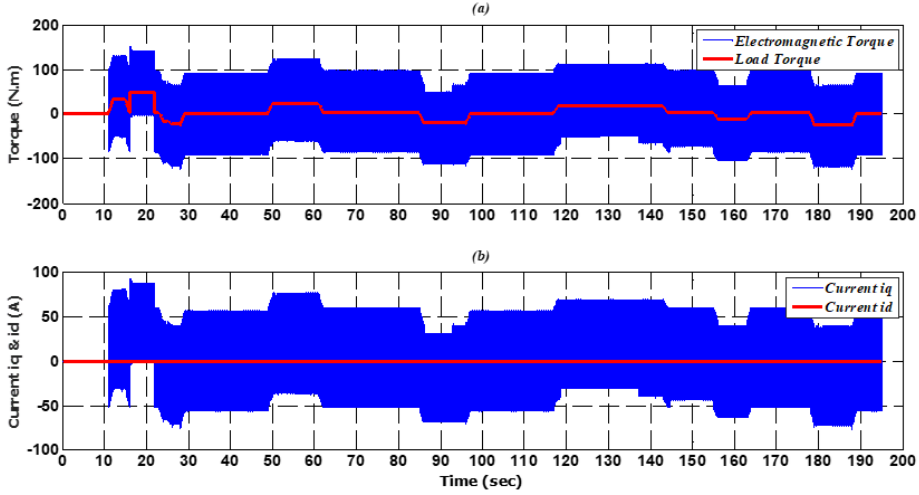

Figure 5. a)Electromagnetic and load torque and (b) quadratic and direct currents in SMC

To show the ANFIS mode controller performances we have simulated the system described above. Figure 4(a) show the vehicle speed response, the rotation speed of the motorcan rapidly track the reference rotation speed , but this control causes fluctuations in the response, it is the phenomenon of chattering (disadvantages of sliding mode control), Figure 4(b) shows the performances of the adaptive neuro-fuzzy controller, acting immediately on the speed loop by a considerable reduce of the chattering phenomenon. Figures 5(a) & 6(c) shows the variation of electromagnetic torque as load torque changes, figures 5(b) & 6(d) illustrates the tow current components quadratic and direct and show good decoupling introduced by PMSM control (the current i_d=0), also the magnitude of q-axis current, iq is proportional to the load torque. Figure.7 shows the three-phase current of the stator.

From figures 5,6 and 7 it can be seen very clear the performances of the adaptative neuro-fuzzy controller , without overflow of the speed, good decoupling and orientation , the phase current have sinusoidal form and remarkably rejection of disturbance.

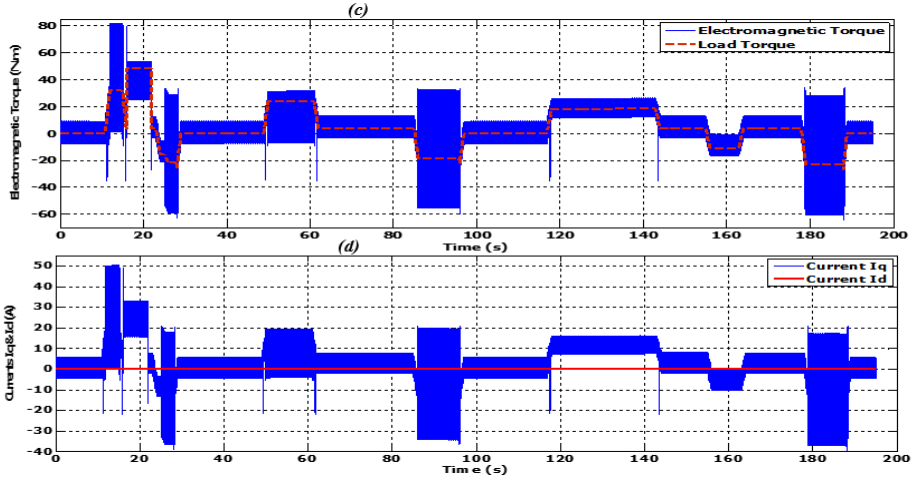

Figure 6. c)Electromagnetic and load torque and (d) quadratic and direct currents in NFSMC

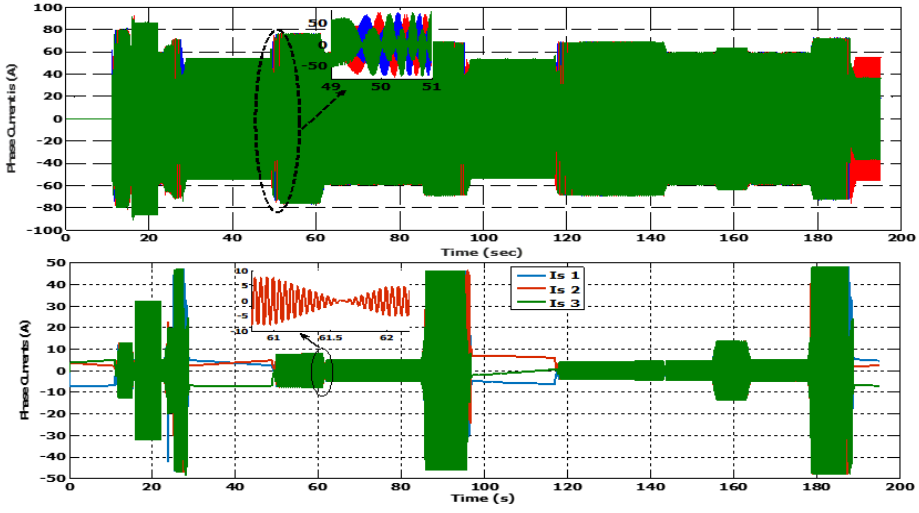

Figure 7.Three phase current is (SMC and NFSMC)

6 Conclusion

The paper presents a strategy based on ANFIS approaches to robust speed control for an electric drive system based on PMSM propulsion . It develops a simple robust controller to deal with parameters uncertain and external disturbances and takes full account of system noise, digital implementation and integral control.

The simulation results show that the proposed controller (NFSMC) is superior to conventional

(SMC) controller in robustness and in tracking precision . The adaptative neuro-fuzzy controller combine the advantages of three modern methods sliding mode SMC,fuzzy logic control FLC, and neural network control. The control of speed by ANFIS gives fast dynamic response indicating the superior performance of adaptive neuro-fuzzy control, because it is inherently adaptative in nature.

References

[1] K. Nam, Y. Hori and C. Lee, " Wheel Slip Control for Improving Traction-Ability and Energy Efficiency of a Personal Electric Vehicle Energies" 2015, 8(7), 6820-6840; doi:10.3390/en8076820

[2] J.S.R. Jang ANFIS: Adaptive-network-based fuzzy inference system, IEEE Trans Syst. Man. Cybernet, 1993; 23(3), pp. 665-85.

[3] J.S.R. Jang, C.T. Sun, E. Mizutani: Neuro-fuzzy and soft computing: A computational approach to learning and machine intelligence, Upper Saddle River, Prentice-Hall, 1997.

[4] A.Tahour , H.Abid, A.Aissaoui," Adaptive Neuro-Fuzzy Controller of Switched Reluctance Motor", SERBIAN JOURNAL OF ELECTRICAL ENGINEERING Vol. 4, No. 1, June 2007, 23–34

[5] C.C. Chan, Y.S. Wong: Electric Vehicles Charge Forward, *IEEE* Power and Energy Magazine, Vol. 2, No. 6, Nov/Dec. 2004, pp. 24 – 33.

[6] Z.Q. Zhu, D. Howe: Electrical Machines and Drives for Electric, Hybrid, and Fuel Cell Vehicles, Proceeding of the IEEE, Vol. 95, No. 4, April 2007, pp. 746 – 765.

[7] M. Vasudevan, R. Arumugam: New Direct Torque Control Scheme of Induction Motor for Electric Vehicles, Asian Control Conference, Melbourne, Australia, Vol. 2, July 2004, pp. 1377 – 1383.

[8] R.F. Fung, C.L. Chiang, G.C. Wu, System identification of a pick-and-place mechanism driven by a permanent magnet synchronous motor, Appl. Math. Model. 34 (2010) 2323–2335.

[9] P. Pillay, R. Krishnan, Modelling of permanent magnet motor drives, *IEEE* Trans. Indust. Electron. 35 (1988) 537–541.

[10] N.K. Yadav and R. K. Singh, "Hybrid Fuzzy Sliding Mode Controller for Timedelay System", International Journal of Artificial Intelligence & Applications (IJAIA), Vol. 4, n°. 4, July 2013.

[11] A.Tahour, A.Hamza , A.Aissaoui :Speed Control of Switched Reluctance Motor using Fuzzy Sliding Mode, Advance in Electrical and Computer Engineering, Vol,8.15,Number 1(29),2008.

[12] C.T.Lin, C.S.G.Lee, neural network based fuzzy logic control and decision systems, IEEE transactions on computers, 40(12):1320-1336, December 1991.

10TH INTERNATIONAL CONFERENCE ON SUSTAINABLE ENERGY AND ENVIRONMENTAL PROTECTION (JUNE 27TH – 30RD, 2017, BLED, SLOVENIA), TECHNICAL DEVELOPMENTS IN VEHICLES
J. Krope, A.Ghani Olabi, D. Goričanec & S. Božičnik

Electronic Differential with Backstepping Control for Vehicle Propulsion System

AHMED LARBAOUI, BEGHDAD BELABBES, IBRAHIM FAROUK BOUGUENNA & AHMED TAHOUR

Abstract This paper proposes a traction drive system for electric vehicles (EVs) with two separate permanent magnet synchronous motor (PMSM) drive-based wheels. Each motor-wheel is supplied by a static converter which is powered by batteries. The two sub systems (source-converter-motor) are coupled to an electronic differential (ED) in order to compensate the tendencies of direction of the vehicle and maintain a steady speed by adjusting the difference in speed of each motor-wheel according to the direction in the case of a turn. In this case, an ED is developed. To handle EV stability while cornering or under slippery road condition, the proposed traction drive uses a nonlinear backstepping control speed. The simulation results with Matlab/Simulink software clearly show the effectiveness of the proposed adaptive ED in terms of can track the speed references robustness and stability.

Keywords: • Permanent Magnet Synchronous Motor (PMSM) • Electric Vehicles (EVs) • Motor-Wheel • Electronic Differential (ED) • Backstepping Control •

CORRESPONDENCE ADDRESS: Ahmed Larbaoui, PhD Student, University of Sidi Bel abbes, Faculty of electrical Engineering, 22000 Sidi Bel Abbes, e-mail: s.godounov@gmail.com. Beghdad Belabbes, Full Professor, University of Sidi Bel abbes , Faculty of electrical Engineering , 22000 Sidi Bel Abbes, e-mail: belabbesbag@yahoo.fr. Ibrahim Farouk Bouguenna, PhD student, University of Sidi Bel abbes , Faculty of electrical Engineering , 22000 Sidi Bel Abbes, e-mail: faroukspvusto@yahoo.fr. Ahmed Tahour, Full Professor, University of Sidi Bel abbes , Faculty of electrical Engineering, 22000 Sidi Bel Abbes, e-mail:tahourahmed@yahoo.fr.

https://doi.org/10.18690/978-961-286-062-2.2 ISBN 978-961-286-062-2

Available at: http://press.um.si.

1 Introduction

The transportation sector is the largest consumer of oil and it has grown at a higher rate than any other sector in recent decades [3]. Increases in transportation have caused pollution emissions because of the utilization of internal combustion engine (ICEs), and that have consequently caused some environmental problems, which must be prevented to maintain the quality of life. Thus, many governments have developed more stringent standards for the pollution emissions of vehicles [4].

In order to achieve better fuel economy and lower emissions, both academia and automotive industry have conducted research on improving the efficiency of powertrains, developing other energy sources, and changing the concept of the conventional powertrains to electric vehicles EVs including EVs, HEVs, and FCVs [5].

Generally, in most electric vehicle (EV) propulsion applications, an ac motor is connected to the wheels by reduction gears and a mechanical differential. in some vehicle drive arrangements, high-speed, low-torque wheel motors requiring gear reduction are used, and in these cases, either a gear motor assembly is mounted inside the wheel, or a chassis mounted motor is connected to the wheel through gear reduction [6][8].

further simplification of the vehicle drive arrangement results in the elimination of the gear being interposed between motor and wheel. the above then calls for the use of an electric differential (ED) [1],[4].

ED-based EVs have advantages over classical EVs with a central motor. Indeed, mounting the motors directly to the wheels simplifies the mechanical layout. The ED system will reduce the drive line components, thus improving the overall reliability and efficiency. This option will also reduce the drive line weight since mechanical differential and gear reduction are not used. However, one of the main issues in the design of these EVs (without mechanical differential) is to ensure vehicle stability in particular while cornering or under slippery road conditions [2]. This calls for a specific traction control system .

The control of the traction effort transmitted by each wheel is at the base of the command strategies aiming to improve the stability of a vehicle. Each wheel is controlled independently by using an electric motorization. However, the traditional thermal motorization always requires the use of a mechanical differential to ensure the distribution of power on each wheel. The mechanical differential usually imposes a balanced transmitted torques, and in the case of an electric traction system, this balance can be obtained by using a dual-motor structure which is shown in Figure 4 [3],[8].

In this context, the PMSM has been adopted as the EV propulsion base. Among the available PMSM control technique, backstepping control is applied to the speed tracking control appears to be very convenient for EV applications [9], [10], [11].

The backstepping design offers a choice of design tools for the accommodation of uncertainties nonlinearities, and can avoid wasteful cancellations. In addition, the backstepping approach is capable of keeping almost all the robustness properties of the mismatched uncertainties [10], [11].

The backstepping is a systematic and recursive design methodology for nonlinear feedback control. The basic idea of backstepping design is to select recursively some appropriate functions of state variables as pseudo control inputs for lower dimension subsystems of the overall system. Each backstepping stage result in a new pseudo control design, expressed in terms of the pseudo control designs from preceding design stages. When the procedure terminates, a feedback design for the true control input results in achieving of a final Lyapunov function by an efficient original design objective. The latter is formed by summing up the Lyapunov function associates with each individual design stage [9].

2 Control of the Electric Differential-Based Electric Vehicle Traction Drive

Figure 3 shows the proposed traction system of an electric vehicle with two independent wheel drives. Two machines thus replace the standard case with a single machine and a differential mechanical. The power structure in this paper is composed of two permanent magnet synchronous motors via fixed gears which are fed by two three-phase inverters and driving the two rear wheels of a vehicle through gearboxes. However, the control method used in this work for the motors with ED is the adaptive backstepping control will give the vehicle a dynamic behavior similar to that imposed by motor with a mechanical differential [1],[2].

The ED system uses the vehicle speed and steering angle as input parameters and calculates the required inner and outer wheel speeds where

the two rear wheels are controlled independently by two PMSM. Figure 3 shows the proposed system control for the electronic differential based on backstepping.

2.1 Vehicle dynamics

Figure 1 shows the forces acting on a vehicle moving up a grade. The total resistive force is defined as

$$F_{res} = F_{rr} + F_{ad} + F_{hc} \tag{1}$$

and

$$F_{rr} = \mu_{rr} mg \tag{2}$$

$$F_{ad} = \frac{1}{2}\rho\, C_{\omega}\, A_f \left(V - V_0\right)^2 \tag{3}$$

$$F_{hc} = \pm\, \frac{1}{2} mg\, \sin\alpha \tag{4}$$

where F_{rr} is the Rolling resistance force, F_{ad} is the Aerodynamic drag, F_{hc} is the hill climbing force

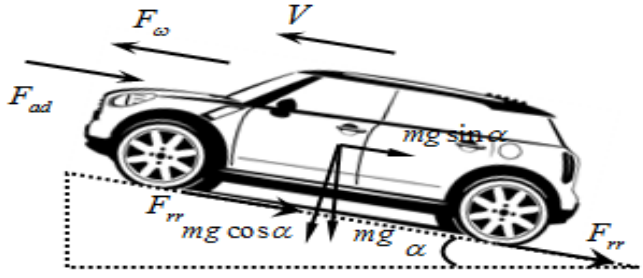

Figure 1. Forces acting on a vehicle

2.2 Modelling the electronic differential

The considered propulsion system architecture permits one to develop an electronic differential to assure that over a straight trajectory the two wheel drives roll exactly at the same velocity; and in a curve trajectory the difference between the two wheel velocities insure the vehicle trajectory over the curve. See Figure 2. Since the two rear wheels are directly driven by two separate motors, If the vehicle is turning right, the left wheel speed is increased and the right wheel speed remains equal to the common reference speed ω_{r_ref} . If the vehicle is turning left, the right wheel speed is increased and the left wheel speed remains equal to the common reference speed ω_{r_ref} [2],[7],[8]. this helps the tyres from losing traction in turns. Figure 2(b) shows the vehicle structure describing a curve, where L represents the wheelbase, δ the steering angle, d the distance between the wheels of the same axle and ω_{r_L} and ω_{r_R} the angular speeds of the left and right wheel drives, respectively.

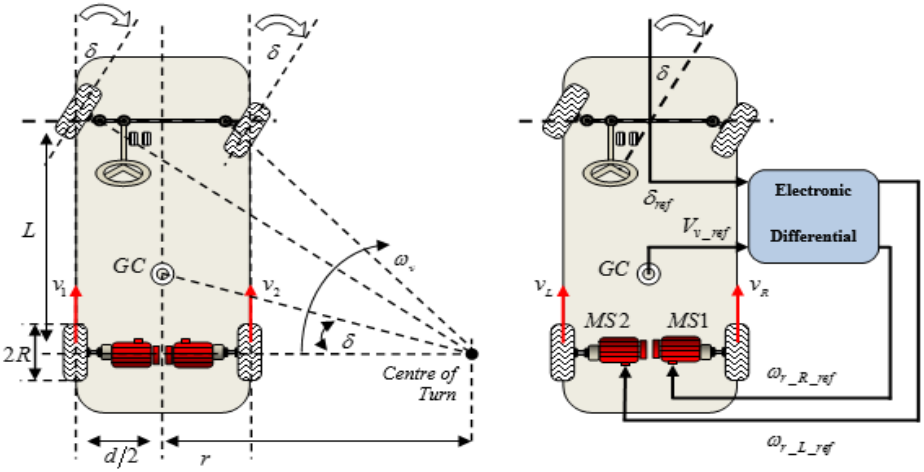

Figure 2 . (a) Structure of electronic differential. (b) Design model for vehicle structure driven

in a curve. The linear speed of each wheel drive is expressed as a function of the vehicle speed and the radius of curve:

$$v_L = \omega_v \left(R + \frac{d}{2} \right) \tag{5}$$

$$v_R = \omega_v \left(R - \frac{d}{2} \right) \tag{6}$$

The curve radius is related to the wheelbase and steering angle:

$$R = \frac{L}{\tan(\delta)} \tag{7}$$

Substituting (7) into Equations (5) and (6), we obtain the angular speed in each wheel drive:

$$\omega_{r_L} = \frac{L + 0.5\, d \tan(\delta)}{L} \omega_v \tag{8}$$

$$\omega_{r_R} = \frac{L - 0.5\, d \tan(\delta)}{L} \omega_v \tag{9}$$

The difference between the angular speeds of the wheel drives is expressed by the relation

$$\Delta\omega = \omega_{r_R} - \omega_{r_L} = \frac{d\tan(\delta)}{L}\ \omega_v \tag{10}$$

Numeric sign of the steering angle signal indicates the curve direction:

$\delta \succ 0 \Rightarrow$ Turn right
$\delta = 0 \Rightarrow$ Straight ahead
$\delta \prec 0 \Rightarrow$ Turn left.

When the vehicle begins a curve, the driver imposes a steering angle to the wheels. The electronic differential however acts immediately on the two motors reducing the speed of the inner wheel and increases the speed of the outer wheel. The driving wheel angular speeds are,

$$\omega_{r\_L\_ref} = \omega_v + \frac{\Delta\omega}{2} \tag{11}$$

$$\omega_{r\_R\_ref} = \omega_v - \frac{\Delta\omega}{2} \tag{12}$$

The speed references of the two motors are:

$$\omega_{Lm\_ref} = k_{gear}\ \omega_{r\_L\_ref} \tag{13}$$

$$\omega_{Rm\_ref} = k_{gear}\ \omega_{r\_R\_ref} \tag{14}$$

Where k_{gear} is the gearbox ratio.

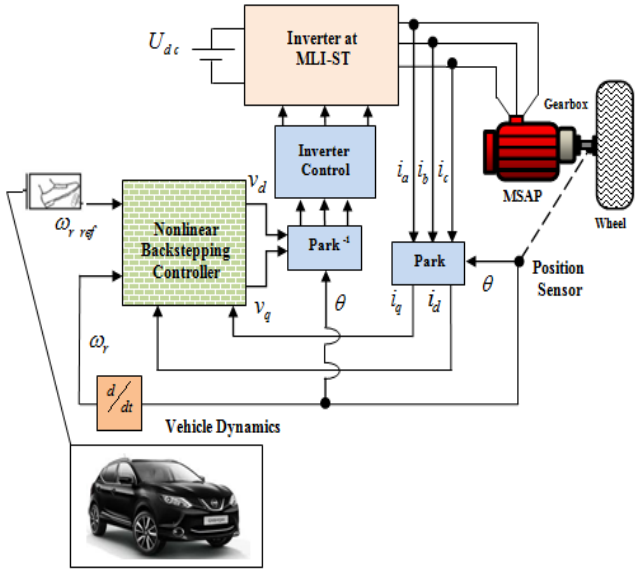

Figure 3 . Electrical traction chain

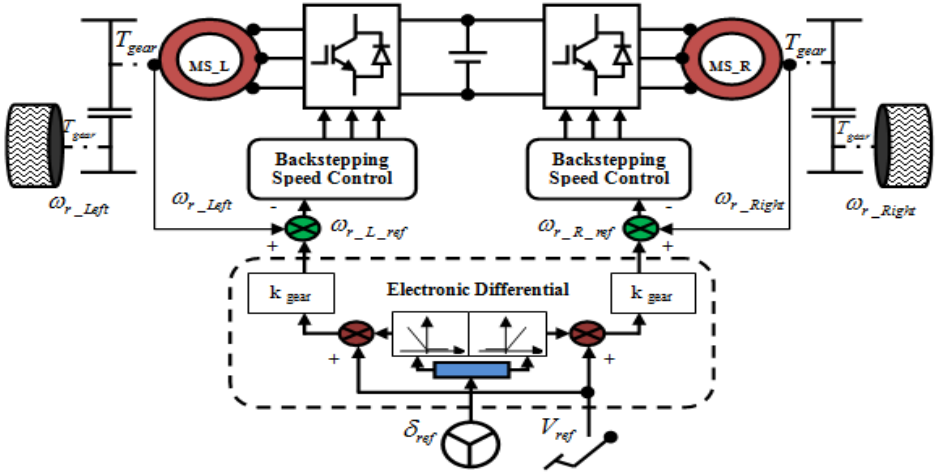

Figure 4. Block diagram show use of the electronic differential.

2.3 Traction motor model

Using Park transformations, the PMSM mathematical model in a rotating reference frame (*d*-*q*), is defined by the following system of Equation. [9]:

With R_s: Stator resistance, L_d , L_q d and q-axis stator inductances, ϕ_f :Permanent-magnet flux linkage, i_d , i_q: Stator currents, v_d , v_q: Stator voltages, ω_r: Speed mechanic, j: Moment of inertia, f: Coefficient of viscous friction, p: Number of pole pairs, T_L :Load torque.

$$\begin{cases} \dot{i}_d = -\dfrac{R_s}{L_d}\, i_d + \dfrac{L_q}{L_d}\, p\ \omega_r\ i_q + \dfrac{v_d}{L_d} \\ \dot{i}_q = -\dfrac{R_s}{L_q}\, i_q - \dfrac{L_d}{L_q}\, p\ \omega_r\ i_d - \dfrac{\phi_f}{L_q} p\ \omega_r + \dfrac{v_q}{L_q} \\ \dot{\omega}_r = \dfrac{3p}{2j}(\phi_f\ i_q + (L_d - L_q) i_d\ i_q) - \dfrac{f}{j}\omega_r + \dfrac{T_L}{j} \end{cases} \tag{15}$$

3 Nonlinear Backstepping Control Design for PMSM

The essence of backstepping is the stabilization of a virtual control state. Hence, it generates a corresponding error variable which can be stabilized by carefully selecting proper control inputs. These inputs can be determined from Lyapunov stability analysis [9],[10]. From Eq. (15), it is obvious that the dynamic model of PMSM is highly nonlinear because of the coupling between the speed and the electrical currents. According to the vector control principle, the direct axis current i_d is always forced to be zero in order to orient all the linkage flux in the d axis and achieve maximum torque per ampere. It is assumed that the engine parameters are known and invariant [11]. The proposed control system is designed to achieve velocity-tracking objective and described step by step as follows.

3.1 Backstepping speed controller

The first step is defined the tracking errors:

$$e_{\omega_r} = \omega_{r\_ref} - \omega_r \tag{16}$$

The derivative of an Equation (16) is
:

$$\dot{e}_{\omega_r} = \dot{\omega}_{r\_ref} - \frac{1}{j}\left[\frac{3p}{2}\left(\phi_f\ i_q + \left(L_d - L_q\right) i_d\ i_q\right) - f\,\omega_r - T_L\right] \tag{17}$$

We define the following quadratic function:

$$V_1 = \frac{1}{2} e_{\omega_r}^2 \tag{18}$$

Its derivative along the solution of Eq. (18), is given by:

$$\begin{aligned} \dot{V}_1 &= \dot{e}_{\omega_r} \; e_{\omega_r} \\ &= \left(\dot{\omega}_{r\_ref} - \frac{1}{j} \left[\frac{3p}{2} \left(\phi_f \; i_q + \left(L_d - L_q \right) i_d \; i_q \right) \right. \right. \\ &\qquad \left. \left. - f \omega_r - T_L \right] \right) e_{\omega_r} \end{aligned} \tag{19}$$

Using the backstepping design method, we consider the *d-q* axes currents components i_d and i_q as our virtual control elements and specify its desired behavior , which are called stabilizing function in the backstepping design terminology as follows:

$$\begin{cases} i_{d\ ref} = 0 \\ i_{q\ ref} = \dfrac{2}{3\,p\,\phi_f} \left(f \omega_r + T_L + j\, k_{\omega_r} e_{\omega_r} \right) \end{cases} \tag{20}$$

With: k_{ω_r} is a positive constant.

Substituting Equation (19) in Equation (18), the derivative of V_1:

$$\dot{V}_1 = -k_{\omega_r} . e_{\omega_r}^2 \leq 0 \tag{21}$$

3.2 Backstepping current controller

We have the asymptotic stability of the origin of the system of Equations. (15).
We defined current following errors:

$$\begin{cases} e_d = i_{d\ ref} - i_d \\ e_q = i_{q\ ref} - i_q \end{cases} \qquad \text{with} \quad i_{d\ ref} = 0 \tag{22}$$

Their dynamics can be written:

$$\dot{e}_d = \dot{i}_{d\ ref} - \dot{i}_d = \frac{R_s}{L_d} i_d - \frac{L_q}{L_d} p\ \omega_r\ i_q - \frac{v_d}{L_d} \tag{23}$$

$$\begin{aligned} e_q &= i_{q\ ref} - i_q \\ &= \frac{2}{3\ p\ \phi_f}\left(f\,\omega_r + T_L + j\ k_{\omega_r} e_{\omega_r} \right) \\ &\quad + \frac{R_s}{L_q} i_q + \frac{L_d}{L_q} p\ \omega_r\ i_d + \frac{\phi_f}{L_q} p\ \omega_r - \frac{v_q}{L_q} \end{aligned} \tag{24}$$

$$\begin{aligned} \dot{e}_q &= \dot{i}_{q\ ref} - \dot{i}_q \\ &= \frac{2\left(k_{\omega_r} j - f\right)}{3 f\ \phi_f}\left(\frac{3p\ \phi_f}{2\,j} e_q + \frac{3p\left(L_d - L_q\right)}{2\,j} e_d i_q \right. \\ &\quad \left. - k_{\omega_r} e_{\omega_r} \right) + \frac{R_s}{L_q} i_q + \frac{L_d}{L_q} p\ \omega_r\ i_d + \frac{\phi_f}{L_q} p\ \omega_r - \frac{v_q}{L_q} \end{aligned} \tag{25}$$

To analyze the stability of this system we propose the following Lyapunov function:

$$V_2 = \frac{1}{2}\left(e_{\omega_r}^2 + e_d^2 + e_q^2\right) \tag{26}$$

To guarantee the global asymptotic stability in the current loop, we must satisfy the following inequality:

$$\dot{V}_2 \le 0 \tag{27}$$

The *d-q* axes control voltages are chosen as follows:

$$\begin{aligned} v_d &= k_d\ L_d\ e_d + \frac{3\,p\left(L_d - L_q\right) L_d}{2\,j} e_{\omega_r} i_q + R_s\ i_d \\ &\quad - p\ \omega_r\ L_q\ i_q \end{aligned} \tag{28}$$

$$v_q = \frac{2\left(k_{\omega_r}\ j - f\right)L_q}{3\ p\ \phi_f}\left(-k_{\omega_r}\ e_{\omega_r} + \frac{3\ p\ \phi_f}{2\ j}e_q + \frac{3\ p\left(L_d - L_q\right)}{2\ j}e_d\ i_q\right) + k_q\ L_q\ e_q + \frac{3\ p\ \phi_f\ L_q}{2\ j}e_{\omega_r} + R_s\ i_q + p\ \omega_r\ L_d\ i_d + p\ \omega_r\ \phi_f \tag{29}$$

Therefore, finally we obtain the following expression of the differentiating Lyapunov function :

$$\dot{V}_2 = -k_{\omega_r} e_{\omega_r}^2 - k_d\ e_d^2 - k_q\ e_q^2 \le 0 \tag{30}$$

4 Simulation Results and Discussion

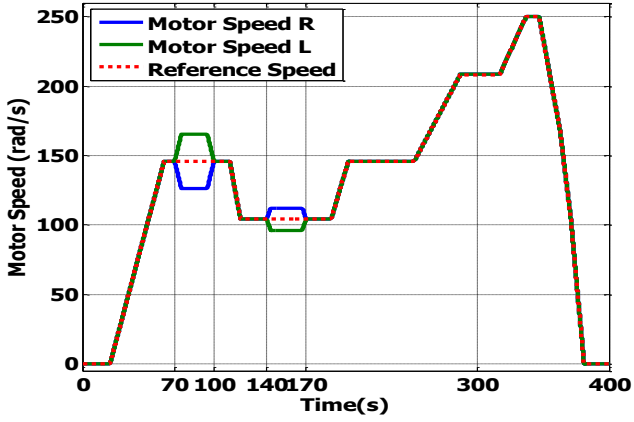

Figure 5. Vehicle wheel speed in different cases

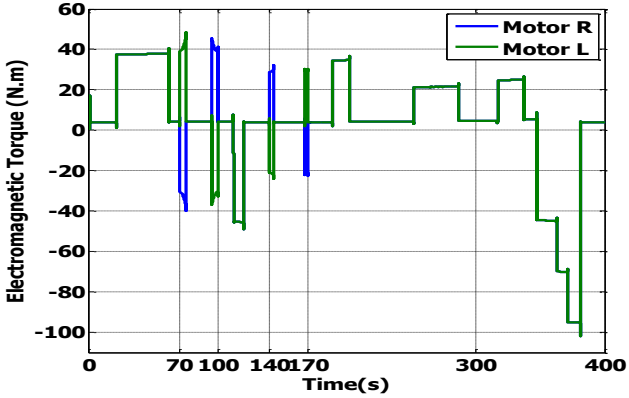

Figure 6. Variation of electromagnetic torque of the right and left motor in different phases

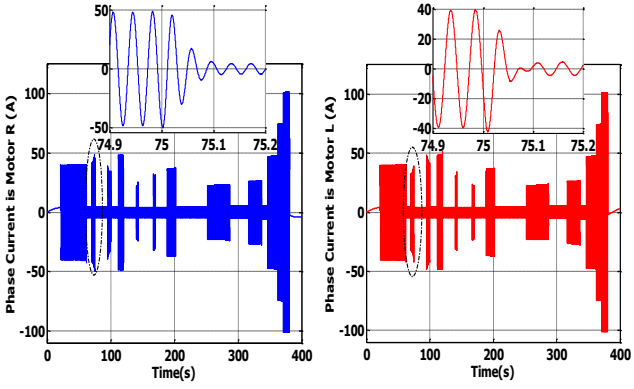

Figure 7. Phase current for motors right and left.

It should be noted that the simulation run under an extra-urban driving cycle (EUDC) figure (5) , which shows each wheel speed during steering for $0 < t < 400$ sec. During this cycle the vehicle approaches a right turn at 70 sec and a left turn at 140 sec .It is obvious that the electric vehicle operates satisfactorily according to the complicated series of accelerations, decelerations, and frequent stops .

Referring to the figure (5) and figure (6), the vehicle turn right at 70 sec, in compensation the torque of the right wheel decreases, briefly becoming negative. Negative torque is, in essence, braking mode. This working phase can be exploited for energy recuperation. Once the speed of the right wheel is stabilized , the torque returns to its initial value, as it is shown in Figure (6). At t= 100 s the vehicle exits the curved section of road; thus the driver applies an inverse steering angle to the front wheels. The electronic differential subsequently acts to equalize the speed of the drive motors; The speed difference of the

driving wheels is shown in figure (5). At 140 sec the vehicle approaches a left turn, it can be seen that the electronic differential acts immediately on both electric motors by lowering the speed of the left wheel and, unlike that on the right. This speed is illustrated in Figure (5). The variation of phase currents are shown in Figure (7).

5 Conclusion

This paper has dealt with an ED based EV. The ED system will reduce the drive line components, thus improving the overall reliability and efficiency since mechanical differential and gear reduction are not used. In this case, The EV traction drive system uses two separate PMSM back drive based wheels.

The proposed ED has been developed to handle the EV stability while cornering or under slippery road conditions. For that purpose, it uses a backstepping speed control .The results obtained by simulation show that this structure allows the design and implementation of an electronic differential and ensures good dynamic and static performances. The paper shows that the electronic differential controls the driving wheels speeds with high accuracy either in flat roads or curved ones. The disturbances do not affect the performances of the driving motors.

References

[1] A. Draou ," A Simplified Sliding Mode Controlled Electronic Differential for an Electric Vehicle with Two Independent Wheel Drives ," Energy and Power Engineering ,2013,vol. 5, pp.416–421, Aug. 2013 .

[2] K. Houacine, R. Mellah and S. Guermah , "Compensatory neural fuzzy control for two wheels electric vehicle drive," International Journal of Electric and Hybrid Vehicles, vol. 7, pp. 189–207, 2015.

[3] B. Tabbache, A. Kheloui, M. Benbouzid ," An Adaptive Electric Differential for Electric Vehicles Motion Stabilization," IEEE Transactions On Vehicular Technology, vol. 60, pp. 104–110, January .2011.

[4] A. Haddoun, M. Benbouzid, D. Diallo, R. Abdessemed, J. Ghouili, K. Srairi , "Design and Implementation of an Electric Differential for Traction Application," Vehicle Power and Propulsion Conference (VPPC), IEEE, 1-3 Sept. 2010.

[5] F. J. Perez-Pinal, I. Cervantes, and A. Emadi, "Stability of an electric differential for traction applications," IEEE Trans. Veh. Technol., vol. 58, pp. 3224–3233, Sep. 2009.

[6] N. Mutoh, Y. Hayano, H. Yahagi, and K. Takita, "Electric braking control methods for electric vehicles with independently driven front and rear wheels," IEEE Trans. Ind. Electron., vol. 54, pp. 1168–1176, Apr. 2007.

[7] M. Sekour, K. Hartani, A. Draou, A. Allali ,"Sensorless Fuzzy Direct Torque Control for High Performance Electric Vehicle with Four In-Wheel Motors," Journal of Electrical Engineering and Technology, Vol. 8, pp. 530–543, May.2013 .

[8] B. Gasbaoui , A. Chaker , A. Laoufi, B. Allaoua , "The efficiency of direct torque control for electric vehicle behavior improvement," Serbian Journal of Electrical Engineering, Vol. 8, pp.127–146, 2010.

[9] R. George , A. S. Mathew .Speed Control of PMSM using Backstepping Method. International Journal of Engineering Research & Technology (IJERT) ,vol. 4 , pp. 609–612 July.2015.

[10] C. X. Chen, Y. X. Xie, Y. H. Lan. Backstepping Control of Speed Sensorless Permanent Magnet Synchronous Motor Based on Slide Model Observer. International Journal of Automation and Computing, vol. 12 , pp. 149–155, April. 2015.

[11] M. Moutchou , A. Abbou , H. Mahmoudı, "MRAS-based sensorless speed backstepping control for induction machine, using a flux sliding mode observer,"Turkish Journal of Electrical Engineering & Computer Sciences, vol. 23, pp. 187 –200, 2015.

10TH INTERNATIONAL CONFERENCE ON SUSTAINABLE ENERGY AND ENVIRONMENTAL PROTECTION (JUNE 27TH – 30TH, 2017, BLED, SLOVENIA), TECHNICAL DEVELOPMENTS IN VEHICLES
J. Krope, A.Ghani Olabi, D. Goričanec & S. Božičnik

Optimization of Automotive Diesel Engine Calibration Using Genetic Algorithm Techniques

FEDERICO MILLO, PRANAV ARYA & FABIO MALLAMO

Abstract The advancements in diesel engines have resulted in possibility of achieving better performance with lower emissions and an increased complexity with a higher number of control parameters, thus requiring the solution of optimization problems of higher dimensionality. It is therefore of crucial importance to identify suitable methodologies, which can allow achieving the full exploitation of the potential of these powertrains. In this paper, a methodology for optimizing the latest generation of common rail automotive diesel engines have been discussed. First, random optimization methods along with surrogate models were used to generate a population of engine calibrations already having good performance in terms of emissions and fuel consumption. Finally, these calibrations served as an initial population to the Genetic Algorithm (GA) based optimizer. The application of the optimizer on a real data set for a particular engine operating point has been presented in the paper. The results from the optimizer showed an impressive reduction in the target quantity.

Keywords: • Engine Calibration • Optimization • Genetic Algorithm • Surrogate Models • Diesel Engines •

CORRESPONDENCE ADDRESS: Federico Millo, Full Professor, Energy Department, Politecnico Di Torino, Corso Duca Degli Abruzzi, 24, Torino, 10129, Italy, email: federico.millo@polito.it. Pranav Arya, Ph.D. Student, Energy Department, Politecnico Di Torino, Corso Duca Degli Abruzzi, 24, Torino, 10129, Italy, email: pranav.arya@polito.it. Fabio Mallamo, Ph.D., Powertrain Engineering Department Manager, FEV Italia s.r.l, Politecnico Di Torino, Corso Duca Degli Abruzzi, 24, Torino, 10129, Italy, e-mail: mallamo@fev.com.

https://doi.org/10.18690/978-961-286-062-2.3 ISBN 978-961-286-062-2

Available at: http://press.um.si.

1 Introduction

The demand for reduction in emissions and better performance from automotive industry has transpired an evolution of diesel engines. This progress, with the assistance of modern common rail fuel injection, turbocharging and aftertreatment systems, has greatly increased the efficiency of the diesel engine [1], [2], [3]. It has also resulted in a better control of the combustion process, with possibilities like injection rate shaping, premixed combustion to further reduce emissions and fuel consumption. This better control also means a higher number of control parameters and complex interactions between different parameters. This makes defining the optimal tuning of these control parameters more complicated and difficult. This tuning of engine control parameters over the complete operating range is referred to as engine calibration.

Calibration of engine consists of using the empirical emission models created by Design of Experiment (DoE) and optimizing the control parameters in order to have a good performance of engine at a particular point. This process is repeated at multiple points to cover the complete operating region of the engine and create maps for the engine control parameters to optimize the performance of the engine. These maps of the control parameters have an additional requirement of smoothness. Of course, it is not possible to create models for all the operating points, it is for this reason some operating points are selected based on their time weight in the driving cycle. These operating points are called Key Points (KP) and they represent a cluster of operating points in their vicinity. This approach is commonly known as the local approach for modelling [4].

With the increase in the number of control parameters, firstly the models that are created need to be more complex in order to represent the combustion process adequately. Use of conventional models like polynomial models is declining, since these models cannot satisfactorily model problems of higher dimensionality. Therefore, black box models based neural networks and Gaussian Process (GP), are being extensively used for modelling applications [5], [6]. These methods have the advantage of being capable of modelling very complicated multi-dimensional non-linear mapping. At the same time, the optimization techniques should be well suited to the modelling methods. Classical numerical techniques of optimization like simple gradient method, steepest decent method worked well with trivial non-convex functions and convex functions [7]. However, they are dependent on the initialization, since they have a tendency to be trapped in local minima. Furthermore, their application is limited on to continuous differentiable functions. GA have been popular because of its stochastic nature and its ability to avoid getting trapped in local minima.

In addition, population based measure such as GA, gives a set of good mathematically feasible solution and not just one solution like conventional methods. If the final solution found by population-based methods, is not feasible due to the problems regarding implementation, then it is always possible to revert to the other good solutions.

2 Engine Emission MOdels

For the purpose of this study, an operating point at 2000 rpm and 5 bar brake mean effective pressure (BMEP) was selected as an example KP. This operating point was selected because it is traditionally optimized in local modelling approaches. The operating points in the vicinity of this key point are frequently encountered during the operation of engine in common driving cycles like NEDC and WLTC.

The models and the data sets used in the study were provided by FEV Italia. GP was used for modelling the emissions at engine out level and fuel consumption as a function of 9 parameters. These parameters were Start of Injection (SOI), Air Quantity, Injection or Rail Pressure (RP), Swirl level, 1st and 2nd Pilot quantity, 1st and 2nd Pilot Dwell Time, Boost or Intake Manifold Pressure.

2.1 Model quality

The responses of the four different models that were used have been shown in Figure 1-4. The normalized experimental value has been plotted on the x-axis and the normalized predicted value from the model on y-axis. The NO_x model was clearly the best in terms of predictions, as it is evident from R^2 coefficient. Soot model showed a predictive capability almost similar to the NO_x model. Combustion Noise (CN) and Brake Specific Fuel Consumption (BSFC) model also showed sufficiently good performance. The four models were extensively tested on the engine test bench and the analysis was carried out further using these models.

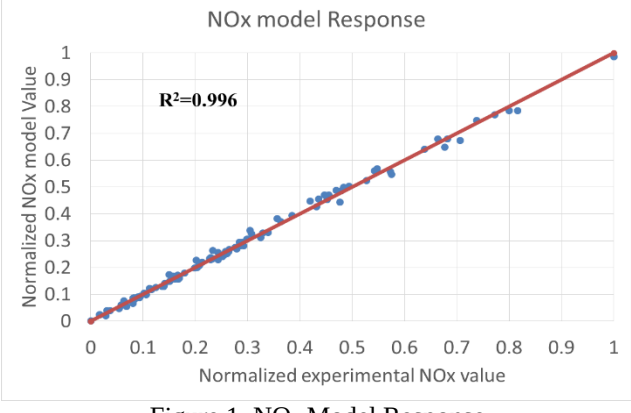

Figure 1. NO_x Model Response

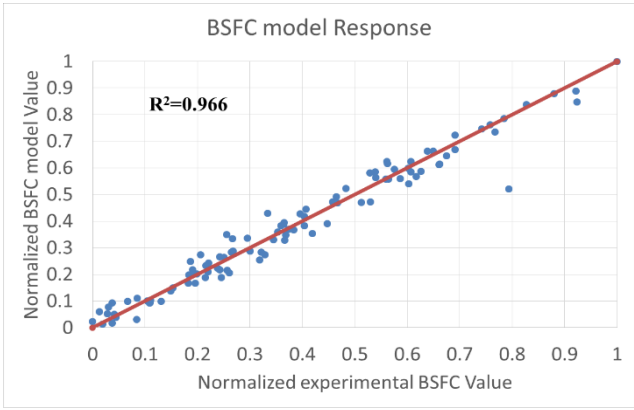

Figure 2. BSFC Model Response

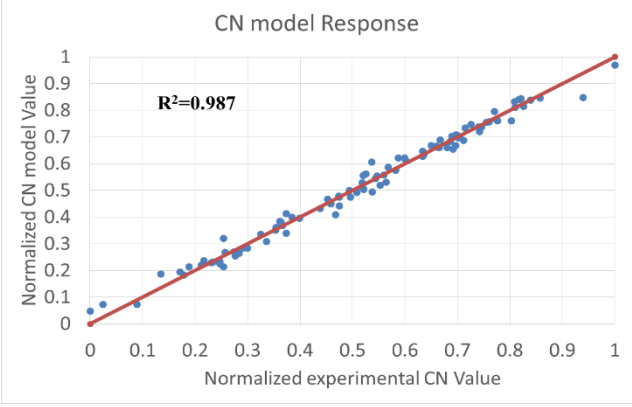

Figure 3. CN Model Response

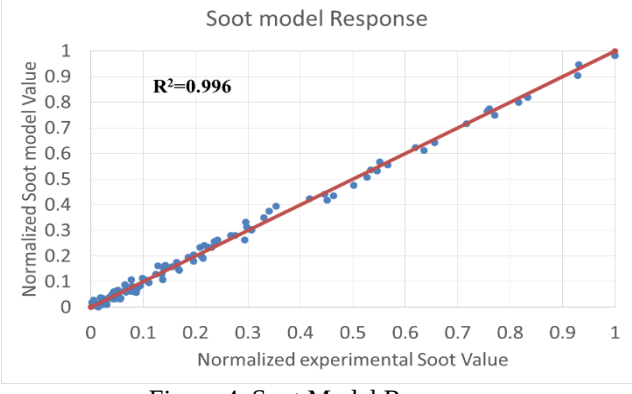

Figure 4. Soot Model Response

2.2 Model domain

For each KP, the DoE is performed in a certain domain i.e. each input parameter in the experiment is varied within a certain range and the models are built with this experimental data. Therefore, the quality of the model is guaranteed only in this domain.

For this study, a pre-existing calibration was already present for the KP. It was assumed that this calibration might already be a good starting point for the optimization. In addition, the calibration of this KP was a part of the calibration of engine in the complete operating range. It means that the maps for the control parameters were already present and were sufficiently smooth.

In order to preserve the smoothness and thus usability of the calibration maps, the models were explored and optimized in a narrow range centered around the pre-existing calibration. The range of variation of models was reduced to 10% of the original domain. As an example, if the DoE was performed with a SOI variation of 0°±4°, then the optimization was restricted to 2°±0.4°, where 2° is the value of SOI in pre-existing calibration. The reduced range of variation of the different control parameters has been shown in Table 1. This also resulted in significant reduction in terms of time and computational power, which has been explained in the next section.

Table 1. Range of variation of the control parameters

Input Quantity	Unit	Range of Variation
Start of Injection	°ATDC	±0.4
Air Quantity	mm^3/stroke	±10
Rail Pressure	MPa	±5
Swirl level	%	±5
1st Pilot Quantity	mm^3/stroke	±0.2
1st Pilot Dwell Time	µs	±100
2nd Pilot Quantity	mm^3/stroke	±0.2
2nd Pilot Dwell Time	µs	±100
Boost Pressure	kPa	±5

3 Optimizer

An in-house optimization code was developed on MATLAB for this study. The code was separated in two main parts, each then having further sub modules. As the GA works with a population of solutions, the first part was the creation of a suitable initial population. This initial population itself resulted in impressive reductions in the targeted quantity. The second step was then further optimization using GA. The two steps have been discussed in detail below:

3.1 Random optimization

For this method, a large number of calibrations within the variation range were generated using random number generator of MATLAB. These calibrations were then evaluated using the GP models. As we narrowed down the variation range, the number of random calibration that were needed to cover the complete range considerably decreased. The constraints for the optimizer were the values of the emissions (NO_x, Soot), CN and BSFC evaluated on the pre-existing calibration using the models. The random calibrations, that resulted in a lower target quantity, without violating the other constraints were stored and the rest of the calibration were discarded. It was ensured that a minimum number of calibrations are stored. In the selected case for this study, NO_x was the target quantity. So the calibrations that resulted in a reduction of NO_x, without increasing the Soot, BSFC or CN were stored. These stored calibrations were then used as an initial population for the genetic algorithm. Figure 5 shows the complete process in a schematic way.

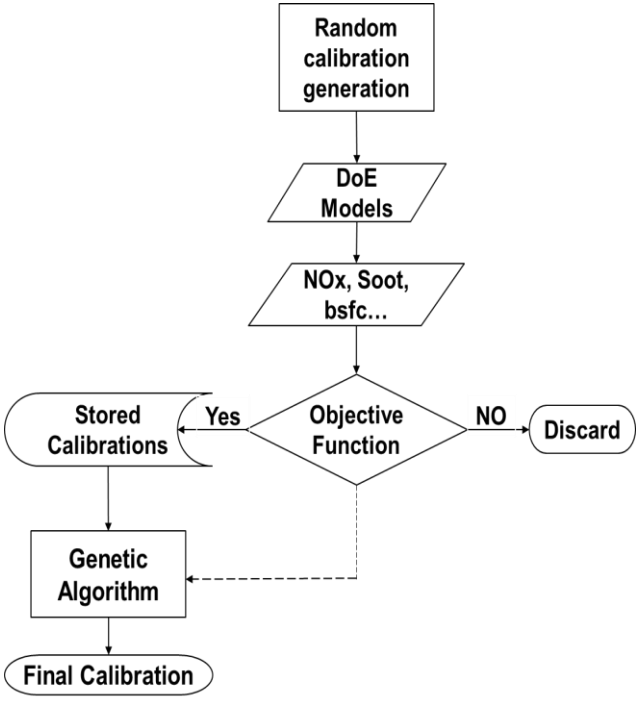

Figure 5. Schematics of the Optimizer

3.2 Genetic algorithm optimizer

Genetic algorithms use the concept of natural selection to find the optimal solution over multiple generations. The number of generations varies from problem to problem. Sastry

et al. describes the steps and working of GA in great detail [8]. However, as the code for GA optimizer was not a commercial one but developed in-house, the modules and working of the optimizer have been described in brief here. Figure 6 shows the various steps in the GA optimizer.

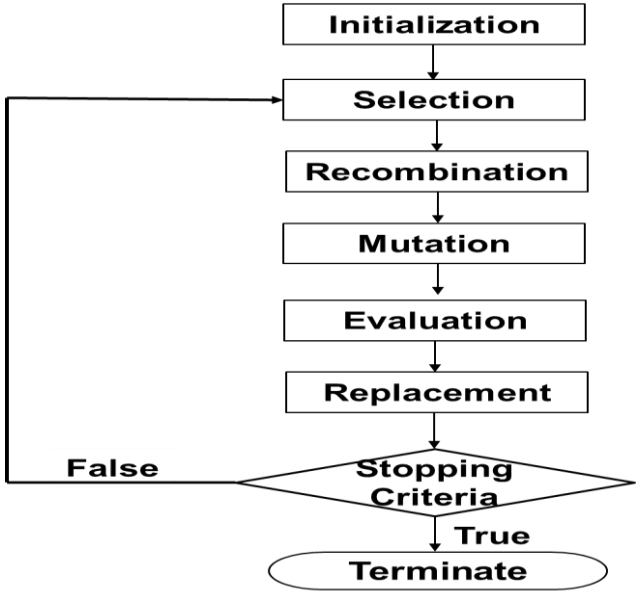

Figure 6. Layout of GA optimizer

Initialization

Each promising solution obtained from the random optimization was first converted in a form of row vector or a string. In terms of GA, each solution in this form is known as a chromosome, each element of this vector is known as gene and the value that these genes take is called allele. In this specific case, the complete calibration was a chromosome, each control parameter was one of the genes and the specific value of that these control parameters take were alleles. The control parameters represented as a chromosome has been shown in figure 7. In the figure, only 7 genes have been shown for the sake of clarity, but in the actual problem the chromosome consisted of 9 genes, same as the number of control parameters. It should be pointed that the number of control parameters depend on the control strategy and can vary a lot depending on the operating point. The methodology explained here can be extended to any number of control parameters.

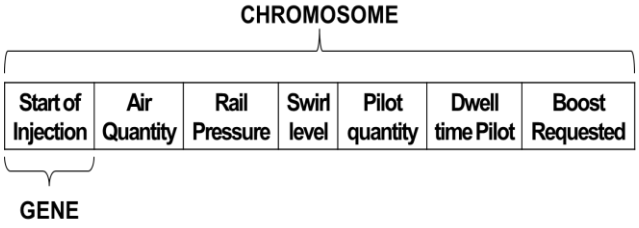

Figure 7. Control parameters represented as a chromosome

Also since, each stored calibration was already evaluated using GP models during the random optimization; a fitness value was assigned to each calibration using equation (1)

$$Fitness = (NO_{x,Base} - NO_{x,i})/NO_{x,Base}. \quad (1)$$

where, $NO_{x,Base}$ is the value of the target quantity obtained from the pre-existing calibration and $NO_{x,i}$ is the value in i^{th} generation.

Selection

From the stored calibrations passed on by random optimizer, 50 calibrations were selected as parents using a roulette wheel method. Since a standard method for selection was chosen, it has not been explained here [9].

Recombination

In recombination, some genes of parent chromosomes are swapped using a certain technique to most likely create more fit children chromosomes. For the optimizer, uniform crossover technique was used, where swapping of each gene is considered separately with a probability of 0.5. The recombination was carried out by generating a row of random bits of same length as the chromosome. Each bit corresponded to a particular gene. If the bit was 0, then the gene was swapped between the parents P1 and P2. If the bit was 1 then the gene of parents P1 and P2 was copied as it is to the children C1 and C2. This has been illustrated more clearly in figure 8. Again the illustration shows 7 genes for the sake of clarity, but actual problem consisted of 9 control parameters.

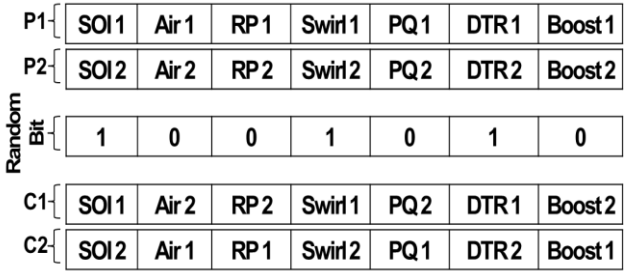

Figure 8. Recombination based on uniform crossover

Mutation

After every 10 generations, one of the 9 genes, was selected at random. This gene was replaced with a value of that control parameter generated randomly within the narrow domain.

Evaluation and Replacement

The outputs (NO_x, Soot, CN, BSFC) were evaluated using the GP models for the new population that was created using recombination and mutation functions. Also, for each chromosome the fitness was calculated using equation (1). If the fitness increased, without violating the same constraints introduced in the random optimizer, then the child chromosome was passed on to the new generation. If there was no increase in the fitness or if any of the constraint was violated, then the parent chromosome was copied to the new generation. This ensured an increase in fitness over the number of generations without increasing any other emissions or fuel consumption.

Stopping Criteria

In this case, the stopping criteria was a fixed number of generations. The GA was run for 200 generations.

4 Results

The methodology explained above has been applied to reduce the NO_x for a pre-existing calibration. Figure 9 shows the NO_x variation relative to the calibrated NO_x generation by generation over the entire 200 generations.

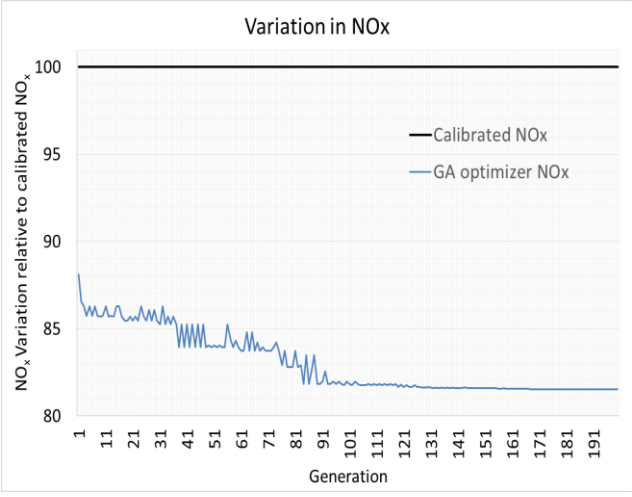

Figure 9. Variation in NO_x

As evident from the figure, a significant part of the total reduction came from the random optimization. This can be more clearly seen from figure 10 which shows the value of fitness increasing over the generations.

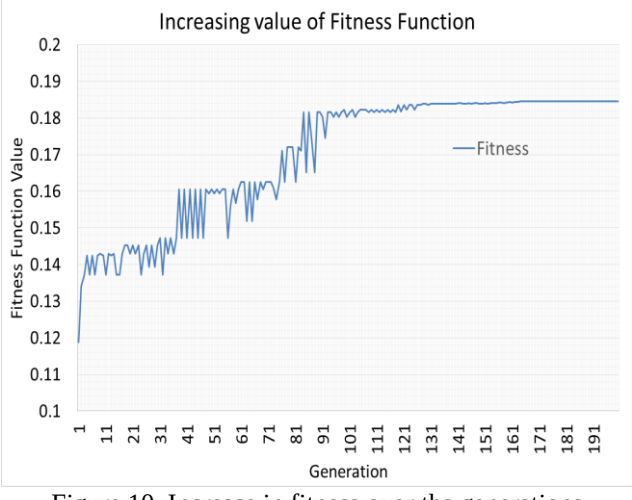

Figure 10. Increase in fitness over the generations

Figure 9 and Figure 10 are complementary in nature. It is because of the selected fitness function given in equation (1) that fitness shown in Figure 10 is also reduction in NO_x relative to calibrated NO_x. As can be seen in figure 10, the plot starts from 0.12 and

reaches almost 0.19. This signifies that roughly 12% reduction came from random optimization and further 7% reduction was achieved because of the GA.

The figure shows the fitness value decreasing for certain generation. This happened because a population was created for a generation because of the crossover and mutation and it was evaluated for the fitness. If the fitness obtained was worse than the previous generation, the algorithm reverted back to the previous population. It is clear from the plot, that for every worsening of the fitness function, the algorithm returns to the same value of the fitness before the worsening.

Figure 11, 12 and 13 shows the CN, Soot and BSFC variations over the generations respectively.

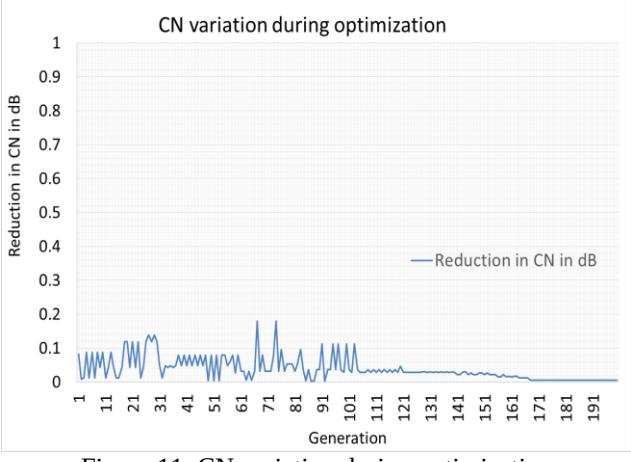

Figure 11. CN variation during optimization

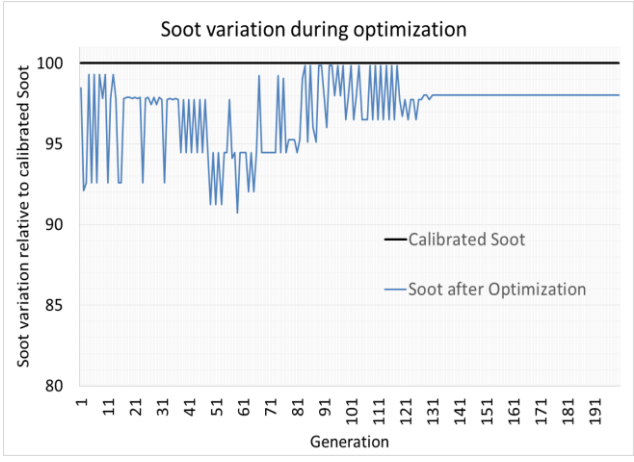

Figure 12. Soot variation during optimization

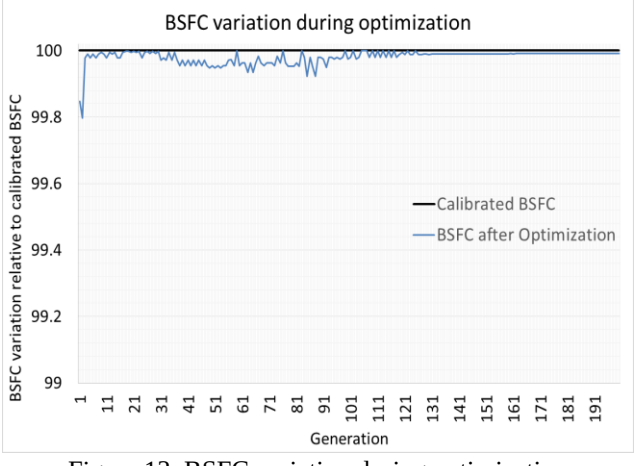

Figure 13. BSFC variation during optimization

It can be identified from the figures that the constraints were not violated in any of the generations. Furthermore, the final values obtained for CN and BSFC are really close to the constraints, as these were not being optimized. It was because the variations in BSFC in Figure 13 could not be identified, that the scale was changed. A significant reduction is only obtained for NO_x, which was the target.

5 Future Work

The application of the optimizer can be further extended to a non trivial application where the pre-existing calibration is not present and hence the narrow constraints are not there.

The range of varation would be the complete domain of the model and an additional step of defining the constraints dynamically would be required.

Furthermore, the optimizer can even be extended to multiple KP's for both the scenarios, with and without pre-existing calibrations. Thus the optimizer can be used to optimize the complete operating range of an engine.

References

[1] W. Knecht, "Diesel engine development in view of reduced emission standards", *Energy*, vol. 33, pp. 264-271, Feb. 2008.

[2] M. Badami, F. Mallamo, F. Millo, and E.E. Rossi, "Experimental investigations on the effect of multiple injection strategies on emissions, noise and brake specific fuel consumption of an automotive direct injection common-rail diesel engine", *International Journal of Engine Research*, vol. 4, pp. 299-314, Aug. 2003.

[3] A.G. Stefanopoulou, I. Kolmanovskz, and J.S. Freudenberg, "Control of variable geometry turbocharged diesel engines for reduced emissions", *IEEE Transactions on Control Systems Technology*, vol. 8, no.4, pp. 733-745, Jul. 2000.

[4] M. Castagne, Y. Bentolila, F. Chaudoye, A.Halle, F. Nicolas, and D. Sinoquet, "Comparison of engine calibration methods based on Design of Experiments (DoE)", *Oil & Gas Science and Technology*, vol. 63, pp. 563-582, 2008.

[5] B. Crack and S. Demirtas, "An application of artificial neural network for predicting engine torque in a biodiesel engine", *American Journal of Energy Research*, vol. 2 No.4 , pp. 74--80, 2014.

[6] B. Berger, F. Rauscher, and B. Lohmann, "Analysing Gaussian processes for stationary black-box combustion engine modelling", *IFAC Proceedings Volumes*, vol. 44, pp. 10633-10640, Jan. 2011.

[7] R. Fletcher and M.J.D. Powell, "A rapidly convergent descent method for minimization", *The Computer Journal*, vol. 6 Issue 2, pp. 163-168, Aug. 1963.

[8] K. Sastry, D. Goldberg, and G. Kendall, "Genetic Algorithms," in *Search Methodologies: Introductory Tutorials in Optimization and Decision Support Techniques*, E. K. Burke and G. Kendall, Eds. Boston, MA: Springer US, 2005, pp. 97–125.

[9] D. E. Goldberg, *Genetic Algorithms in Search, Optimization, and Machine Learning*, Addison Wesley Reading MA, 1989.

10TH INTERNATIONAL CONFERENCE ON SUSTAINABLE ENERGY AND ENVIRONMENTAL PROTECTION (JUNE 27TH – 30TH, 2017, BLED, SLOVENIA), TECHNICAL DEVELOPMENTS IN VEHICLES
J. Krope, A.Ghani Olabi, D. Goričanec & S. Božičnik

Hydraulic Transmission for Agricultural Machine Appropriate for the Treatment of Steep Farmland

MARTIN KODRIČ & STANISLAV PEHAN

Abstract The paper presents the conceiving and designing of a hydraulic transmission for an agricultural machine suitable for treatment of steep farmland. For moving the machine upwards and downwards, it is required to distribute the engine power to the correct branch, wheels and/or rope, which represents the major problem. Another problem occurs when the agricultural machine runs two accessories, requiring stable power at input. The machine is equipped with an engine, which is as small as possible with the aim of causing minimal ground damage. The analysis of different transmission systems leads to the conclusion that the hydraulic transmission is the best choice. It fulfils all the requirements concerning the lowest weight. The appropriate piping diagrams of the hydraulic scheme are developed and accompanied with adequate analytical calculations. A prototype of the machine is made and its operation is tested. Practical tests confirm the rightness of using the hydraulic transmission.

Keywords: • hydraulic • transmission • agricultural machine • steep terrain •

CORRESPONDENCE ADDRESS: Martin Kodrič, Ph.D., Krško, Nuclear power Plant, Vrbina 12, 8270 Krško, Slovenia, e-mail: martin.kodric@nek.si. Stanislav Pehan, Ph.D., Associate Professor, University of Maribor, Faculty of Mechanical Engineering, Smetanova ulica 17, 2000 Maribor, Slovenia, e-mail: stanislav.pehan@um.si.

https://doi.org/10.18690/978-961-286-062-2.4 ISBN 978-961-286-062-2

Available at: http://press.um.si.

1 Introduction

For the treatment of the sloped terrain planted with permanent crops and inclined at angles greater than 60%, winch power is required [1]. The winch mounted on the reef of the terrain pulls the cart with the accessories upwards. For this design, two motors are required: one runs the winch, whereas the other runs the accessories. This arrangement works on a steep terrain only. The obvious disadvantage is the disability of reusing the potential energy. For the treatment of a flat and sloped terrain, inclined at angles less than 60%, classic tractors with wheels or tracks are in common use [2], [3] and [4]. In case of a mixed structure of the terrain, where flat segments are included, a new agricultural treatment method should be introduced, with the cart being substituted with a self-propelled machine with the winch [5]. Approaches for an effective power transmission design are investigated, with the aim to conceive a small and light agricultural machine that would enable simultaneous operation of two accessories.

2 Hydraulic Transmission

The basic motor of the machine is a small internal combustion diesel engine. The criterion for the determination of the engine power is the climbing abilities of the machines. The machine transmission consists of two main units. The first one is the wheel drive and the second one is the winch with the anchoring rope, Figure 1.

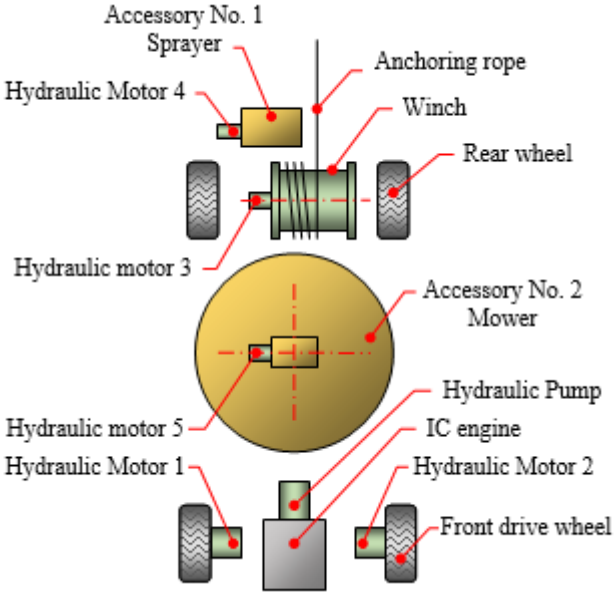

Figure 1. The Layout of the Main Components of the Agricultural Machine

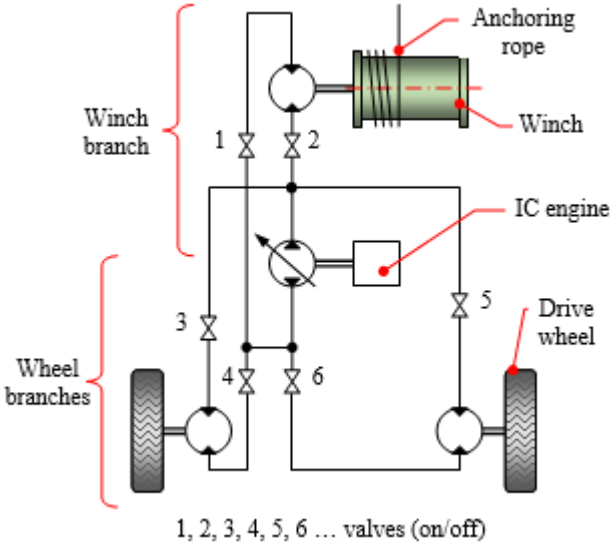

Figure 2. Basic Hydraulic Transmission

The minimum configuration of necessary hydraulic components, presented in Figure 2, can operate successfully in case that both driving systems are independent and the valves 1 to 6 are opened. The basic hydraulic transmission actually represents a kind of differential, which operates well in normal conditions but once the wheels slip, the winch becomes useless, and also with no power. Consequently, when driving the machine upwards on a slippery terrain, both wheel branches should be switched off. When driving the machine downwards, the winch or both wheel branches could be switched off. It means that the valves on input and output pipes of a pertinent hydraulic motor should be closed and that would transform this motor into a blocked brake. As a result, the machine would stop. To avoid this, the hydraulic transmission should be modified.

2.1 Hydraulic circuit designing

To enable the rotation of each of the switched off hydraulic motors, the free circuit of the hydraulic fluid should be enabled. This can be done by introducing additional valves, numbered 7, 8 and 9 in Figure 3. In such a case the hydraulic motor, which is switched off, operates as a pump pushing the flow inside a closed local circuit. For example, while only the winch drive operates, the valves 3, 4, 5, 6 and 7 are closed and the valves 1, 2, 8 and 9 are open, Figure 3. Also by the switched off circuit due to the previous operating conditions, the high pressure in the piping still exists and causes harmful resistances, which leads to power loss that heats the hydraulic system.

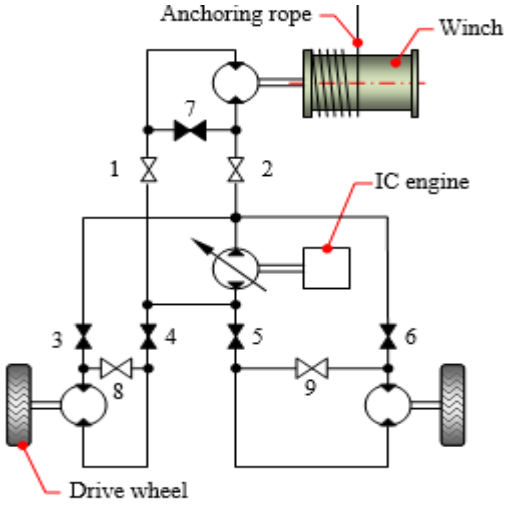

Figure 3. Closed Hydraulic Circuit

To overcome this disadvantage of a closed circuit, the open circuit is introduced, Figure 4.

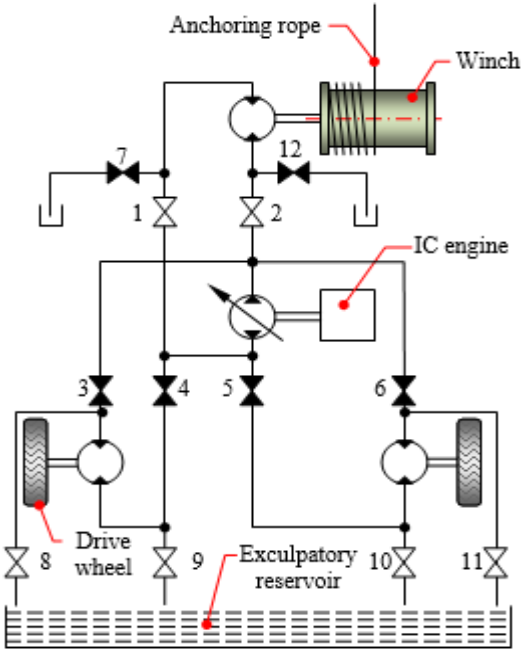

Figure 4. Open Hydraulic Circuit

The most prominent component of the open hydraulic circuit is the exculpatory reservoir. The inlet and outlet pipes of each hydraulic motor are connected with it. In case of operating the winch drive only, the valves 3, 4, 5, 6, 7 and 12 are closed and the valves 1, 2, 8, 9, 10 and 11 are open. The hydraulic fluid in both wheel branches can now freely circulate at the atmospheric pressure and at a negligibly low resistance. The hydraulic fluid freely circulates from the reservoir through the hydraulic motor, which acts as pump, and returns back into the reservoir with a symbolic resistance only.

2.2 Hydraulic drives for accessories

The accessories can be driven by the IC engine or by potential energy obtained from the hydraulic system, Figure 5. The accessories operate when the machine goes downwards and the potential energy comes from the winch rope, which rotates the additional pump producing the energy in the hydraulic system. The potential energy obtained from the winch is sufficient for one accessory only. The energy for the other accessory is obtained from the IC engine.

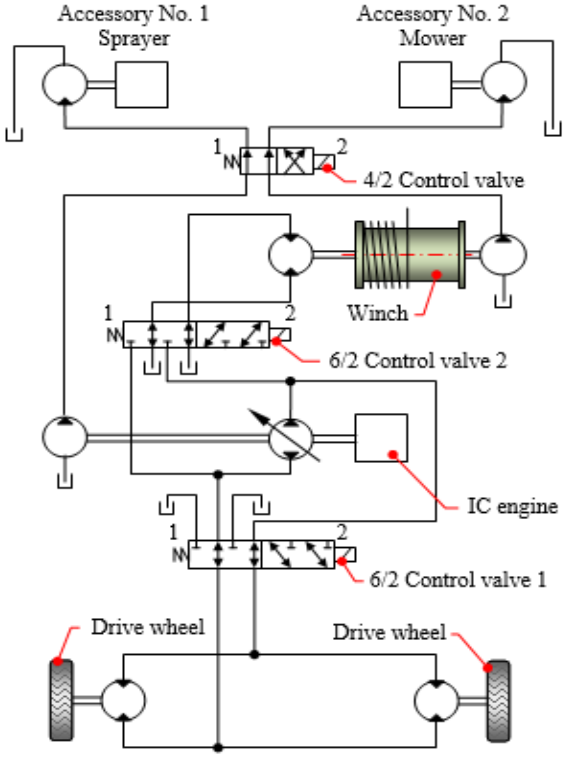

Figure 5. Hydraulic Circuit of the Agricultural Machine for Driving and for Crop Treatment

The major advantage of the presented hydraulic system is its ability to combine the two energy sources and to transform their energy into proper input torque and rpm adequate for accessories. The 4/2 control valve makes it possible to select the accessories. Figure 5 shows a situation with the machine travelling downwards. Both accessories operate. The winch is operated with the open hydraulic circuit. The machine speed is adjusted with the drive wheels. When the vehicle moves upwards, it is necessary to activate the winch by moving the control valve 2 from position 1 to position 2. If the drive wheels slip, the control valve 1 must be moved from position 1 to position 2. In this case, the drive wheels rotate in an open hydraulic circuit and the vehicle moves due to the pulling force of the winch.

3 Machine Prototipe Testing

The main purpose of testing is to verify the hypothesis that the hydraulic resistance depends on the pressure in the pipeline. The prototype of the machine is made and some hydraulic properties are tested, Figure 6.

Figure 6. Testing Layout

The influence of the pressure in the hydraulic circuit for winch is tested. The test rig consists of a hand hydraulic pump, which is connected by piping and appropriate hand valves to the real winch with the hydraulic motor MS 100 and gearbox with the speed reduction of 6.2. The nominal diameter of the winch drum is 273 mm. The rope diameter is 5 mm. The resistance of the closed hydraulic circuit is tested first. The winch is driven by a hydraulic hand pump. The valves 1 and 2 are opened, whereas the valve 3 is closed. The valves 1 and 2 are suddenly closed, the valve 3 is opened, and then the tangential force on the winch drum is measured. Tests are carried out at several pressures that gradually increase up to 60 bars. With the same equipment, an open hydraulic circuit is tested. In this case, the valves 1 and 2 are opened, the valve 3 is closed. By the hand pump, the pressure in the system is again raised to the normal level required to drive the winch. Immediately after stopping the hand pump, the pressure in the pipelines drops to the atmospheric level. The tangential force in the pulling rope is measured.

4 Results

The agricultural machine is manufactured in accordance with the presented premise and the hydraulic system transmits the power from the IC engine to individual components. Losses in the hydraulic circuits are manifested in the form of forces and torques needed for the rotation only. The advantage of the open hydraulic circuit is shown in Figure 7. Based on the measured pulling force, the adequate power loss P is calculated. It is considered that the machine is moving at the speed of 5 km/h.

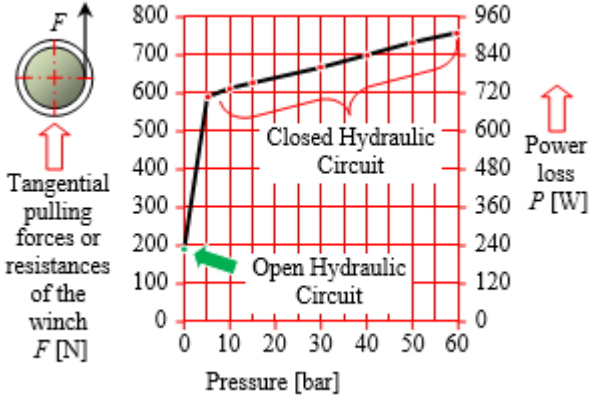

Figure 7. Hydraulic Circuit Resistances

5 Discussion

Rough principles of operation of hydraulic systems are presented; hydraulic schemes of a real machine are much more complex. Measurements of hydraulic resistance on the

winch drive are presented, but the situation is completely identical with respect to all other hydraulic motors and pumps; this machine contains eight. Considering that the nominal values of pressure in the hydraulic system amounts to up to 140 bars, it can be concluded that an open hydraulic circuit significantly reduces the heating of the system.

References

[1] A. Bohme, Umweltgerechte Technik den Steillagenweinbau. KTBL, Darmstadt, 2003.
[2] R. Bernik, Techniques in Agriculture (in Slovenian). Biotechnical Faculty, Department of Agronomy, 2004.
[3] R. Vidoni, M. Bietresato, A. Gasparetto, F. Mazetto. Evaluation and stability comparsion of different vehicle configurations for robotic agricultural operations on side slopes. Biosystems Engineering, vol. 129, pp. 197□211, 2015.
[4] K. Hrastar, Tractor Catalogue: Handbook (in Slovenian). Ljubljana: published by ČZD Kmečki glas, 2014.
[5] M. Kodrič, Development of a hybrid machine for working on sloping terrain (in Slovenian), Doctoral Thesis, University of Maribor, 2016.
[6] T. Katrašnik, F. Trenc, S. Oprešnik, Study of the Energy-Conversion Efficiency of Hybrid Powertrains. Strojniški vestnik □ Journal of Mechanical Engineering, vol. 53, no. 10, pp. 667□682, 2007.
[7] A. Akers, M. Gassman, R. Smith, Hydraulic Power System Analysis, Iowa State University, USA 2006.
[8] J. Flašker, S. Pehan, Power Transmissions: Textbook (in Slovenian). Maribor: Faculty of Mechanical Engineering, 2005.
[9] M. Kodrič, J. Flašker, S. Pehan, Efficiency Improvement of Agricultural Winch Machines. Strojniški vestnik □ Journal of Mechanical Engineering, vol. 63, pp.171□180, Mar. 2017.


METTLER TOLEDO
PRINSIS
energetika ljubljana